The Greenhouse Gas Budget of Terrestrial Ecosystems in East Asia Since 2000

Xuhui Wang, Yuanyi Gao, Sujong Jeong, Akihiko Ito, Ana Bastos, Benjamin Poulter, Yilong Wang, Philippe Ciais, Hanqin Tian, Wenping Yuan, et al.

Global Biogeochemical Cycles®

RESEARCH ARTICLE
10.1029/2023GB007865

The Greenhouse Gas Budget of Terrestrial Ecosystems in East Asia Since 2000

Xuhui Wang[1], Yuanyi Gao[1], Sujong Jeong[2], Akihiko Ito[3], Ana Bastos[4], Benjamin Poulter[5,6], Yilong Wang[7], Philippe Ciais[8], Hanqin Tian[9], Wenping Yuan[10], Naveen Chandra[11], Frédéric Chevallier[8], Lei Fan[12], Songbai Hong[1], Ronny Lauerwald[13], Wei Li[14], Zhengyang Lin[1], Naiqing Pan[15], Prabir K. Patra[11,16], Shushi Peng[1], Lishan Ran[17], Yuxing Sang[1], Stephen Sitch[18], Maki Takashi[19], Rona Louise Thompson[20], Chenzhi Wang[1], Kai Wang[1], Tao Wang[21], Yi Xi[1,8], Liang Xu[22], Yanzi Yan[1], Jeongmin Yun[23], Yao Zhang[1], Yuzhong Zhang[24,25], Zhen Zhang[26], Bo Zheng[27], Feng Zhou[1], Shu Tao[1], Josep G. Canadell[28], and Shilong Piao[1]

[1]College of Urban and Environmental Sciences, Institute of Carbon Neutrality, Sino-French Institute for Earth System Sciences, Peking University, Beijing, China, [2]Department of Environmental Planning, Graduate School of Environmental Studies, Seoul National University, Seoul, South Korea, [3]National Institute for Environmental Studies, Tsukuba, Japan, [4]Department of Biogeochemical Integration, Max Planck Institute for Biogeochemistry, Jena, Germany, [5]Institute on Ecosystems and the Department of Ecology, Montana State University, Bozeman, MT, USA, [6]Biospheric Science Laboratory, NASA Goddard Space Flight Center, Greenbelt, MD, USA, [7]Key Laboratory of Land Surface Pattern and Simulation, Institute of Geographical Sciences and Natural Resources Research, Chinese Academy of Sciences, Beijing, China, [8]Laboratoire des Sciences du Climat et de l'Environnement, LSCE/IPSL, CEA-CNRS-UVSQ, Université Paris-Saclay, Palaiseau, France, [9]Department of Earth and Environmental Sciences, Schiller Institute for Integrated Science and Society, Boston College, Chestnut Hill, MA, USA, [10]School of Atmospheric Sciences, SUN YAT-SEN University, Guangzhou, China, [11]Japan Agency for Marine-Earth Science and Technology (JAMSTEC), Yokohama, Japan, [12]School of Geographical Sciences, Chongqing Jinfo Mountain Karst Ecosystem National Observation and Research Station, Southwest University, Chongqing, China, [13]Université Paris-Saclay, INRAE, AgroParisTech, UMR ECOSYS, Thiverval-Grignon, France, [14]Department of Earth System Science, Tsinghua University, Beijing, China, [15]Department of Earth and Environmental Sciences, Boston College, Schiller Institute for Integrated Science and Society, Chestnut Hill, PA, USA, [16]Research Institute for Humanity and Nature (RIHN), Kamigamo, Kyoto, Japan, [17]Department of Geography, The University of Hong Kong, Hong Kong, China, [18]Faculty of Environment, Science and Economy, University of Exeter, Exeter, UK, [19]Department of Atmosphere, Ocean and Earth System Modeling Research, Meteorological Research Institute, Japan Meteorological Agency, Tsukuba, Japan, [20]Norsk Institutt for Luftforskning, Kjeller, Norway, [21]Department of Civil and Environmental Engineering, The Hong Kong Polytechnic University, Hong Kong, China, [22]Pachama, Inc, San Francisco, CA, USA, [23]Jet Propulsion Laboratory, California Institute of Technology, Pasadena, CA, USA, [24]Key Laboratory of Coastal Environment and Resources of Zhejiang Province, School of Engineering, Westlake University, Hangzhou, China, [25]Institute of Advanced Technology, Westlake Institute for Advanced Study, Hangzhou, China, [26]Department of Geographical Sciences, University of Maryland, College Park, MD, USA, [27]Shenzhen International Graduate School, Institute of Environment and Ecology, Tsinghua University, Shenzhen, China, [28]CSIRO Environment, Canberra, CAN, Australia

Key Points:

- A comprehensive greenhouse gas (CO_2, CH_4 and N_2O) accounting including about 40 flux terms over East Asia is reported
- Terrestrial ecosystems in East Asia are close to greenhouse gas neutral
- Natural ecosystems is a net greenhouse gas sink, compensated by a net source from agricultural ecosystems

Supporting Information:

Supporting Information may be found in the online version of this article.

Correspondence to:

X. Wang,
xuhui.wang@pku.edu.cn

Citation:

Wang, X., Gao, Y., Jeong, S., Ito, A., Bastos, A., Poulter, B., et al. (2024). The greenhouse gas budget of terrestrial ecosystems in East Asia since 2000. *Global Biogeochemical Cycles*, *38*, e2023GB007865. https://doi.org/10.1029/2023GB007865

Received 31 MAY 2023
Accepted 25 JAN 2024

Abstract East Asia (China, Japan, Koreas, and Mongolia) has been the world's economic engine over at least the past two decades, exhibiting a rapid increase in fossil fuel emissions of greenhouse gases (GHGs) and has expressed the recent ambition to achieve climate neutrality by mid-century. However, the GHG balance of its terrestrial ecosystems remains poorly constrained. Here, we present a synthesis of the three most important long-lived greenhouse gases (CO_2, CH_4, and N_2O) budgets over East Asia during the decades of 2000s and 2010s, following a dual constraint approach. We estimate that terrestrial ecosystems in East Asia is close to neutrality of GHGs, with a magnitude of between -46.3 ± 505.9 Tg CO_2eq yr^{-1} (the top-down approach) and -36.1 ± 207.1 Tg CO_2eq yr^{-1} (the bottom-up approach) during 2000–2019. This net GHG sink includes a large land CO_2 sink (-1229.3 ± 430.9 Tg CO_2 yr^{-1} based on the top-down approach and -1353.8 ± 158.5 Tg CO_2 yr^{-1} based on the bottom-up approach) being offset by biogenic CH_4 and N_2O emissions, predominantly coming from the agricultural sectors. Emerging data sources and modeling capacities have helped achieve agreement between the top-down and bottom-up approaches, but sizable uncertainties remain in several flux terms. For example, the reported CO_2 flux from land use and land cover change varies from a net source of more than 300 Tg CO_2 yr^{-1} to a net sink of ~ -700 Tg CO_2 yr^{-1}. Although terrestrial ecosystems over East Asia is close to GHG neutral currently, curbing agricultural GHG emissions and additional afforestation and forest

managements have the potential to transform the terrestrial ecosystems into a net GHG sink, which would help in realizing East Asian countries' ambitions to achieve climate neutrality.

Plain Language Summary East Asia (China, Japan, Koreas and Mongolia) is not only the hotspot of anthropogenic greenhouse gas (GHG, including CO_2, CH_4 and N_2O) emissions, but also a region with large CO_2 sink. However, the greenhouse gas balance of greenhouse gases over the region is poorly understood. In this study, we performed a synthesis for over 40 flux terms to provide the first-of-its-kind GHG budget assessment over the decades of 2000s and 2010s. We find terrestrial ecosystems in East Asia is close to neutrality of GHGs. The bottom-up approach summing up component fluxes estimated a net balance of -36.1 ± 207.1 Tg CO_2eq yr^{-1}, while the top-down approach based on atmospheric inversions estimated a net balance of -46.3 ± 505.9 Tg CO_2eq yr^{-1}. This results from compensation of the large CO_2 sink by CH_4 and N_2O emissions, and from compensation of net GHG sink over natural ecosystems by net GHG source over agricultural ecosystems. Thus, curbing agricultural GHG emissions has the potential to realizing the ambitious goal of achieving climate neutrality over East Asia.

1. Introduction

Over the past two decades, about 30% of anthropogenic CO_2 emissions have been absorbed by terrestrial ecosystems globally (Friedlingstein et al., 2022). Both atmospheric inversions and Dynamic Global Vegetation Models (DGVMs) show that the northern hemisphere contributes the most to the global land CO_2 sink (Stephens et al., 2007; Tagesson et al., 2020), but inconsistencies between the two approaches become larger since the turn of the century (Ciais et al., 2019). However, the northern hemisphere regions and carbon cycle components responsible for the discrepancies remain unclear. One hypothesis attributes part of the discrepancy to the world's largest ever afforestation in China (e.g., Chen et al., 2019, whose impacts on the carbon sink have not yet been well captured by current DGVMs used in global carbon budget assessments (Piao et al., 2018; Pugh et al., 2019; Yu et al., 2022; Yue et al., 2020). This also fuels recent debates on whether there is a stronger land CO_2 sink over East Asia than over the rest of northern hemisphere regions (Piao et al., 2022; J. Wang et al., 2020; Y. Wang et al., 2022). The REgional Carbon Cycle Assessment and Processes, Phase 2 (RECCAP-2) helps to fill the gap by providing consistent methodologies across all northern hemisphere regions and the rest of the world, with this study focusing on GHG budget accounting over East Asia. This effort will help major countries in this region (China, Japan, and Koreas) to assess and track the land CO_2 sink in the pathways of achieving carbon neutrality.

Although CO_2 is the primary GHG responsible for global warming since the preindustrial era, the contribution of CH_4 and N_2O are appreciable, together they highly affect the climate system with global warming potentials that are 27 and 273 times greater than CO_2 at a 100 years time horizon (IPCC, 2021). The GHG budget, including CO_2, CH_4, and N_2O, is thus more relevant to assess the role of the terrestrial ecosystems in mitigating climate change. There is emerging evidence that terrestrial ecosystems could be a net source of GHGs due to emissions of CH_4 and N_2O from both natural and anthropogenic sources (Tian et al., 2016). This is particularly the case for East Asia, given the high intensity of anthropogenic activities which may lead to emission of CH_4 and N_2O from ecosystems (e.g., high nitrogen fertilizer application rate (Cui et al., 2021; Tian et al., 2020), high nitrogen deposition rate (Yu, Jia, et al., 2019), large area of rice paddy fields (Zhang et al., 2016; Figure 1)). However, a knowledge gap remains to be filled in the net GHG budget of East Asia, undermining the region's ambition to manage the ecosystems for mitigating climate change.

In this study, we present a new assessment of the GHG budget of East Asia, with an accounting scheme following the guidelines of RECCAP-2 (Bastos et al., 2022; Ciais et al., 2022) and adapted to the regional characteristics and data availability in East Asia. The GHG budget is constrained both by observation-based assessments from inversions of atmospheric measurements of GHG mixing ratios ("top-down" approach hereafter) and by land-based assessments based on inventories and model simulations of carbon storage change and model estimates of GHG fluxes ("bottom-up" approach hereafter).

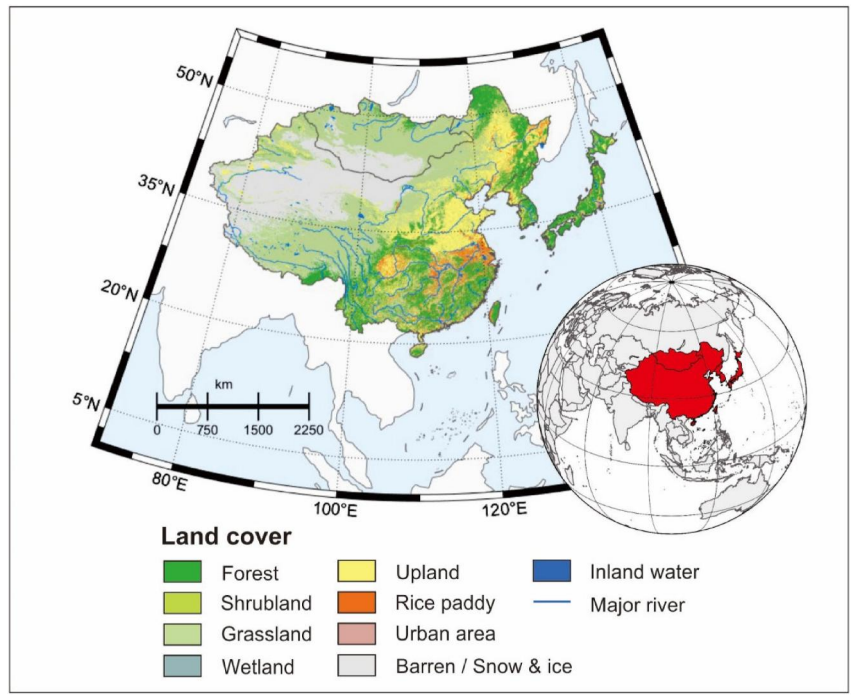

Figure 1. Geographical location and land cover type of East Asia.

2. Methods

2.1. Study Area

Our study area focused on East Asia according to the RECCAP-2 regional division (Ciais et al., 2022), defined as the landmass including China, Japan, the Republic of Korea, the Democratic People's Republic of Korea, and Mongolia. The land area of East Asia is ~1.2×10^7 km^2, occupying ~8% of global land area. Ecosystems in this study include ecosystems such as forests, grasslands, shrublands, croplands, as well as wetlands and inland waters such as rivers, lakes and reservoirs.

2.2. Accounting Framework of the GHG Budget

The framework to assess the ecosystems GHG budget is adapted from the RECCAP-2 proposal, which contains a set of shared and agreed definitions that are as precise as possible for each CO_2 flux to be reported. Compared to RECCAP-1, we aim to provide a synthesis of GHG budget for East Asia since 2000, including three major GHGs (CO_2, CH_4, and N_2O). We updated our accounting framework to GHG budget on the basis of carbon budget from Ciais et al. (2022), which is depicted in Figure 2.

We recommend that our GHG budget is strictly speaking from ecosystems, the effect of fossil fuel combustion, cement production, industry, geological processes (e.g., volcanic eruption), waste and landfills (hereafter called "non-biosphere emissions" for simplicity) should be removed from the total budget. It can be captured by the top-down estimates of CO_2, CH_4, and N_2O flux excluding non-biosphere GHG emissions. The regional CO_2 budget includes CO_2 fluxes resulting from land cover and land use change, climate change and variability, rising atmospheric CO_2, biomass burning, and nitrogen deposition. Bottom-up approaches encompass various methods to quantify regional CO_2 budgets and their component fluxes. The CO_2 budget can be captured by the net carbon stock change of land ecosystems in a region (ΔC in Figure 2), which can be obtained by repeated measurements of live biomass, dead organic matter, soil carbon and by carbon stock change in wood and crop products. The CH_4 budget includes agricultural emissions produced by enteric fermentation, manure management, rice cultivation (included in "agricultural soil" in our framework), aquaculture, and burning of crop residues. Other fluxes include emissions from fire, inland waters, natural wetlands, termites, as well as methane oxidation from natural soil. The N_2O budget includes those released from agricultural ecosystems, that is, fertilized soil emission, manure

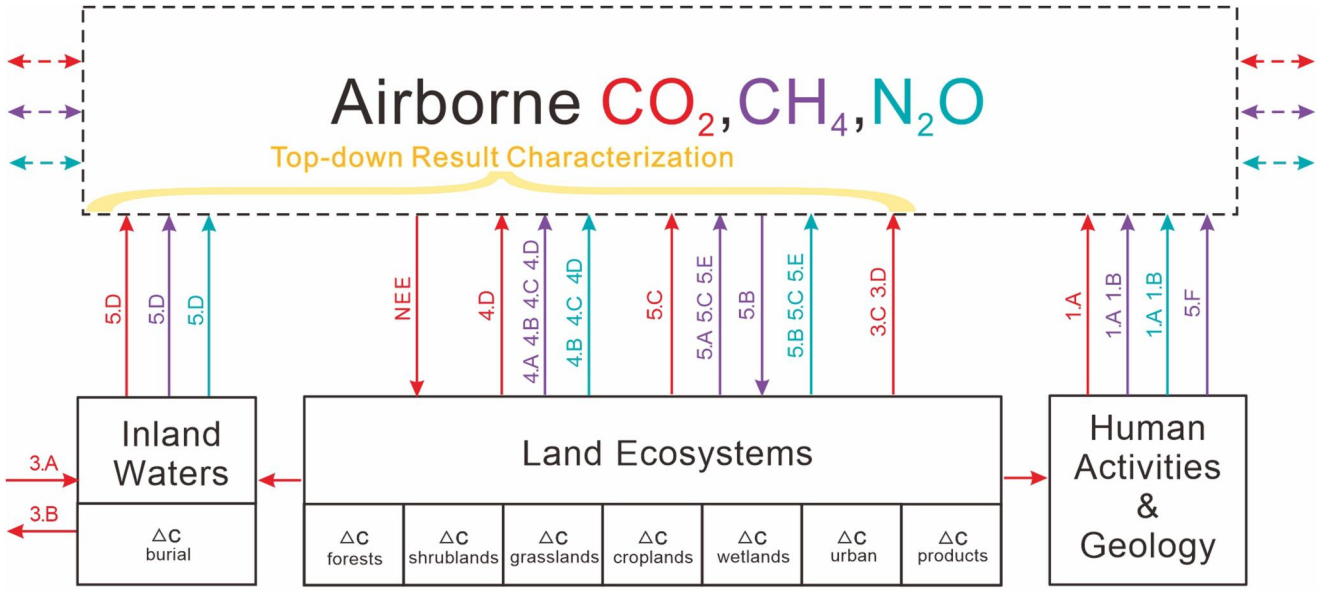

Flux Name			
1. Human activities	2.F Urban Construction	3.C Fossil Fuel RCC	5.B Natural Soil
1.A Fossil Fuel	2.G Burial	3.D Biogenic RCC	5.C Fires
1.B Waste and Landfill	2.H Wood Products	**4. Agriculture**	5.D Inland Waters
2. Carbon Stock Change	**Flux perspective**	4.A Enteric Fermentation	5.E Termites
2.A Forests	Net Ecosystem Exchange	4.B Manure Management	5.F Geological Seepage
2.B Shrublands	Land Cover and Land Use Change	4.C Agricultural Soil	TD inversions
2.C Grasslands	**3. Lateral**	4.D Aqualculture	**Terrestrial Budget**
2.D Croplands	3.A Net Trade	**5. Other Sectors**	BU sink
2.E Wetlands	3.B Lateral Transport to Ocean	5.A Wetlands	TD sink

Figure 2. Accounting framework of the greenhouse gas balance with dual constraints. Flux terms included in the top-down approach indicated by the yellow brace. Bottom-up estimates of the three greenhouse gas fluxes is shown in color arrows (CO_2 (red), CH_4 (purple), and N_2O (blue)). The horizontal arrow indicates lateral flux, the vertical arrow indicates source/sink (upward/downward) of greenhouse gas to the atmosphere, the double arrows refer to the interaction of the gases inside and outside the regional atmospheric boundaries.

management, indirect N_2O emission from manure and synthetic nitrogen fertilizer use, and aquaculture. Sectors from natural ecosystems include emissions from natural soil, inland waters, as well from fire.

To characterize the GHG budget in East Asia, we integrated data separately from bottom-up and top-down approaches with rigorous quantification of the uncertainties, providing a synthesized GHG budget including all terms of GHG fluxes. The estimated budget will better serve as the baseline for climate change mitigation efforts, such as emission reductions and the land-based climate solutions. Data and methods we used are described in the following sections, accessible links of data are available in Supporting Information S1 (Tables S1–S3).

2.3. CO_2

2.3.1. Top-Down Approach

The top-down approach combines measurements of CO_2 mole fractions with atmospheric transport models to constrain the magnitude and location of the combined total surface CO_2 fluxes from all sources (Friedlingstein et al., 2022). In this study, seven atmospheric inversions were used to infer the top-down estimates of the land–atmosphere CO_2 flux for East Asia. For China, three inversion estimates using additional territorial observations

were also included (Chen et al., 2021; Jiang et al., 2016; Y. Wang et al., 2022). To reconcile top-down and bottom-up results, additional adjustments about reduced carbon compounds (RCC, include fossil fuel RCC and biogenic RCC) has been made.

Although fossil fuel CO_2 emissions is not included in the ecosystem GHG budget, it accounts for the largest share of CO_2 emissions and acts as the prior flux in inversion-based CO_2 budget estimate. The fossil fuel CO_2 emissions estimated in this study followed the definition boundary described in the latest GCB (Global Carbon Budget, Friedlingstein et al., 2022). Global inventories (CDIAC-FF, Gilfillan & Marland, 2021; EDGARv7.0, Crippa et al., 2022; CEDSv2021_04_21, Hoesly et al., 2018, McDuffie et al., 2020; PRIMAP-hist, Gütschow et al., 2021, Gütschow et al., 2016) and regional specific datasets (CEADs, GIR, 2021; Long et al., 2020; NCCC, 2010, 2018; NIES, 2022; Shan et al., 2018, 2020) were also taken into our estimation (See more details in the Text S1 in Supporting Information S1).

2.3.2. Bottom-Up Approach

2.3.2.1. Carbon Stock Change

The magnitude of the terrestrial CO_2 balance is driven by multiple processes, which can be quantified by the annual carbon stock changes (ΔC) (Luo et al., 2015). We estimated the ΔC in East Asia since 2000 as the sum of inventory-satellite-model based estimates from above-ground and below-ground carbon storage changes in different ecosystems pools (e.g., forests, grasslands, croplands, others) and other natural carbon stocks (carbon burials in sediments and crop and wood products). IPCC has published useful inventory methods for estimating GHG emissions, here, regionally distributed activity information and statistics are combined with technology-specific emission factors (EF). The methods are categorized into Tier 1, 2 or 3 approaches (IPCC, 2019). Tier 1 represents the simplest approach that relies on default emission factors drawn from previous studies. Tier 2 and Tier 3 methods are based on more nuanced, nationally derived information, while Tier 3 could incorporate more sophisticated approaches, including models and temporally and spatially resolved activity data. More detailed description of the methods of each ΔC can be found in the Texts S2–S7 in Supporting Information S1.

2.3.2.2. Ecosystem Modeling Estimates

The terrestrial carbon budget estimated by the carbon cycle models consists of two parts, the net ecosystem exchange (NEE) and the land cover and land use change flux (Fluc).

We estimated the NEE of East Asia from the TRENDY v9 dataset. More detailed description can be found in the Text S8 in Supporting Information S1. For the Fluc, six estimates, including three bookkeeping approaches, the BLUE (Hansis et al., 2015), OSCAR (Gasser et al., 2020), and H&N2017 (Houghton & Nassikas, 2017); three data-based or model-based approaches, an average estimate derived from 18 dynamic global vegetation models (TRENDY), a process-based model estimate forced by a Chinese land cover dataset by Yu et al. (2022) and a process-based model estimate driven by high resolution satellite land cover maps (Leng et al., under review) were used to estimate the net flux of Fluc in East Asia. Considering the TRENDY models and Hansis et al. (2015) were driven by a common land use forcing (LUH2, Chini et al., 2021), which in contrast to ground-based and satellite evidence of land cover change in China (e.g., Yu et al., 2022) shows increasing cropland area and decreasing forest area, we only took the average from H&N2017, OSCAR, Yu et al. (2022) and Leng et al. (under review) for China. More detailed description can be found in the Text S9 in Supporting Information S1.

2.3.2.3. Lateral Fluxes

Wood and food trade (Ftrade): Ftrade is the net lateral flux of crop and wood products related to trade across the boundaries of each region, calculated as the sum of the export and import fluxes of crop and wood products. For East Asia, we referred to the estimate from Ciais et al. (2021). They estimated the lateral flux of crop products based on the FAO database and Peters et al. (2012) for different forestry products for 2000s. For China, in an analogous manner, Wang et al. (2022) updated the value during 2010–2016. Jiang et al. (2016) estimated the Ftrade based on the import and export data of crop and wood products from the FAO statistical databases. We calculated the average of the two estimates mentioned above to represent Ftrade flux in China.

Carbon export by rivers (Fexport): The river export of carbon delivered to the ocean and across the boundaries of the region includes dissolved organic carbon (DOC), dissolved inorganic carbon (DIC) and particulate organic

carbon (POC). For East Asia, RECCAP-1 estimated the lateral export of carbon involved in terrestrial biological carbon cycling (i.e., excluding the inputs from mineral dissolution given by the difference DIC-DICuptake by chemical rock weathering). The DOC and POC were derived from GlobalNEWS2 (Mayorga et al., 2010), DIC and DICatm (it represents the CO_2 uptake by chemical rock weathering) were derived from Hartmann et al. (2009).

For China, we calculated the mean result from three different methods. (a) We used the RECCAP-1 estimate mentioned above. (b) We used the estimate from Jiang et al. (2016) that based on the observations and empirical formula from previous studies, they estimated Fexport of nine Chinese exorheic rivers during 2006–2009. (c) We used a recent data-driven model estimate (Yan et al., 2023) of DOC export from land to oceans, which applied machine learning methods and a comprehensive set of natural and anthropogenic drivers. Based on Yan et al. (2023)'s estimate and the mean DIC/DOC and POC/DOC ratios observed in the nine rivers from Jiang et al. (2016), we calculated the total carbon exported through the southeast boundaries of East Asia.

2.3.2.4. Other Natural Sectors

Inland waters outgassing (Fwater): The flooding of large stocks of terrestrial organic matter into inland waters may fuel microbial decomposition, converting the organic matter stored in above and below ground biomass to CO_2. The CO_2 outgassing from inland waters in East Asia is calculated in four types of waters: rivers, natural lakes (lake type 1), reservoirs (lake type 2) and lakes regulated by dam (lake type 3). For East Asia, 11 global literature estimates have been synthesized in RECCAP-2, all fluxes are rescaled to consistent estimates of surface area of lakes and reservoirs (after HydroLAKES, Messager et al. (2016)) and rivers (Allen & Pavelsky, 2018). They were further corrected for effects of seasonal ice-cover and ice out (Lauerwald et al., 2023).

Fire CO_2 emissions (Ffire): Two datasets of carbon emissions from fire were collected in our study, the fourth version of the Global Fire Emissions Database (GFED4.1s, Van Der Werf et al. (2017)) and the Live Vegetation Biomass Carbon for the 21st Century (LVBC, Xu et al., 2021). GFED4.1s combined satellite information on fire activity and vegetation productivity to estimate gridded monthly burned area and fire emissions of different fire types: boreal forest fires, temperature forest fires, tropical forest fires, peat fires and agricultural waste burning. LVBC made a conservative estimate of fire emissions separately for forest and non-forest areas by combining Landsat-based forest cover change product and the Moderate Resolution Imaging Spectroradiometer (MODIS) burned area product to avoid the overestimation in confusing the partial clearing from fire with the total clearing in Landsat forest cover change algorithm. We calculated the average of these two estimates for East Asia during 2000–2019.

2.4. CH_4 and N_2O

2.4.1. Top-Down Inversions

For CH_4, we included seven global inversions as described in the global carbon project (GCP; Saunois et al., 2020). These inversions were performed for periods during 2000–2017 using surface and/or satellite observations. Satellite GOSAT retrievals were available only after 2009. Our study also included the updated MIROC4-ACTM (Chandra et al., 2021) and CAMS v20r2_surface inversion results (Arjo et al., 2020). In addition to satellite and surface data that have been assimilated in the above global inversions, we also included results from a regional inversion by Zhang, Fang, et al. (2022) who additionally assimilated surface methane measurements from seven CMA sites across China. They quantified methane emissions during 2010–2017 in East Asia and found that these new data improved the constraints on methane emissions at the sub-regional level. The non-biosphere emissions (induced from fossil fuel, geology, waste and landfills) were subtracted in our final top-down estimate (see Equation 2).

For N_2O, as described in Tian et al. (2020) a total of four estimates from four independent atmospheric inversion frameworks were used in GCP, including GEOSCHEM, INVICAT, MIROC4-ACTM, PyVAR_CAMS. The latest versions which go extend until to 2019 were used in this study. The signal from fossil fuel emissions was removed at the post-processing stage from the inversions mentioned above. We additionally removed the emissions from fossil fuel and waste and landfills in our final top-down estimate (see Equation 3). The average result (including emissions from natural ecosystems and agricultural ecosystems) from the above four estimates since 2000 has been calculated for East Asia.

For the CH_4 and N_2O emissions from fossil fuel and industry, the latest versions of three global datasets: EDGAR, CEDS and PRIMAP-HIST were used to estimate emissions related to fossil fuel and industry. National inventories the NCCC, NIES, and GIR were also included. Non-CO_2 emissions from waste and landfills includes emissions from managed and non-managed landfills (solid waste disposal on land), and wastewater handling, where all kinds of waste are deposited (Saunois et al., 2020). Data from four global inventories were taken into consideration for East Asia (CEDS, GAINS, EDGAR, PRIMAP-HISP), country-level estimates from NCCC, NIES, and GIR were also included.

2.4.2. Bottom-Up Methods

2.4.2.1. Agriculture

While agriculture sectors include a large variety of activities, in practice these sectors were categorized into emissions from enteric fermentation (only CH_4 emissions), manure management, agricultural soils (CH_4 emissions mainly from rice paddies and N_2O emissions mainly from upland soils) and aquaculture.

Enteric fermentation (Fenteric): CH_4 emissions from enteric fermentation accounts for the majority (~90%) of global CH_4 emissions from livestock (Caro et al., 2014; Kumari et al., 2020; Tubiello, 2019). Ruminants represent the main source of the emissions in most countries, especially for China and Mongolia, this flux would be substantial. Three global emission inventories, one regional inventory, and available national inventory reports have been used in this study. The global estimates included FAOSTAT (2022), the EDGARv7.0 (Crippa et al., 2022), and CEDS (v2021_04_21) (Hoesly et al., 2018; McDuffie et al., 2020). The above three inventories are derived using a bottom-up approach where emissions are estimated using reported activity data and source- and region-specific (where available) emission factors. (a) FAOSTAT jointly disseminates the emissions reported by countries to the United Nations Framework Convention on Climate Change (UNFCCC). Estimates are computed at Tier 1 following the IPCC Guidelines for National GHG Inventories from activities located within FAO. (b) EDGAR follows the IPCC (2006) methodology, with FAO (2021) crop and livestock data, specified as livestock numbers for buffalo, camels, dairy and non-dairy cattle, goats, horses, swine, sheep, mules, asses and poultry (turkeys, geese, chickens, and ducks). The livestock populations and cultivated areas rely on FAO activity data are further disaggregated according to different technologies and processes. Where available, nationally, regionally or tailored technology based on Tier 2 emission factors are implemented in EDGAR, and in their absence, default Tier 1 emission factors from IPCC guidelines (IPCC, 2006, 2019) are used. (c) CEDS aims to improve upon existing inventories with a more consistent and reproducible methodology applied to all emissions species, updated emission factors, and recent estimates from 1960 through 2019. It implements a process whereby default emissions were taken directly from national inventories, gap-filled over time using EDGAR estimates with population data from United Nations (UN). CH_4 emissions from enteric fermentation are estimated in nine livestock species: cattle, buffalo, sheep, goats, camels, horses, asses, and swine. For East Asia, Zhang, Tian, et al. (2021) estimated CH_4 emissions from 10 categories of livestock in East Asia during 1961–2019 following the Tier 2 approaches suggested by the 2019 Refinement to the IPCC (2006) Guidelines. For China, Japan and Korea, the national GHG reports NCCC, NIES, and GIR were also collected, respectively.

Manure management (Fmanure): In the case of nonruminant CH_4 emissions, there are about 970 million domestic swine in the world, and nearly half of them are in China (FAO, 2021). The large swine population produces considerable amounts of CH_4 emissions through manure production and management processes (Xu et al., 2019; Zhang, Tian, et al., 2021). We synthesized the estimates from the latest CEDS, EDGAR and FAOSTAT datasets, national inventories NCCC, NIES and and Zhang, Tian, et al. (2021) for this sector.

N_2O emissions from livestock mainly derived from manure management, including livestock excretion, outdoor/grazing, housing, storage, treatment and field application, are considered to produce N_2O. In addition to the datasets mentioned above, here we also used a combination of datasets, the Potsdam Real-time Integrated Model for probabilistic Assessment of emissions Paths (PRIMAP-HIST) emission series (Gütschow et al., 2016). The PRIMAP-HIST dataset combined several published datasets to create two comprehensive sets (HISTCR and HISTTP) of GHG emission pathways from the years 1850–2018. Different priorities are given depending on the data types. In HISTCR scenario, country-reported data (CRF, BUR, UNFCCC) is prioritized over third party data (CDIAC, FAO, Andrew, EDGAR, BP). In HISTTP scenario, third-party data (CDIAC, FAO, Andrew, EDGAR, BP) is prioritized over country-reported data (CRF, BUR, UNFCCC). Both sets were used in this study. For country-scale estimates, in addition to the national GHG report NCCC, NIES and GIR, we included an estimate

made for China from Xu et al. (2022), which used the NUtrient flows in Food chains, Environment and Resources use (NUFER) model and the principle of mass balance method with county-level activity data and N_2O emissions from 1978 to 2016 from province-level activity data and province-specific EFs. This estimate is close to the IPCC Tier 3 approach. Four models (DELM, ORCHIDEE, ORCHIDEECNP, VISIT) simulation results from NMIP project (Tian et al., 2018) were also used in this study.

Agricultural soils (Fagrisoil): Rice cultivation is a major source of CH_4 as most of the world's rice is grown in flooded paddy fields (Qiu, 2009). The estimates of CH_4 emissions from agricultural soils in this study were obtained from five inventory results (the latest CEDS, EDGAR, FAOSTAT, PRIMAP-HISP and The U.S. Environmental Protection Agency (EPA, 2021)), and two model estimates from VISIT (Ito, 2021) are considered for the comparative purpose. EPA provides non-CO_2 GHG emissions based on a Tier 1 methodology. Activity data for rice cultivation included rice area harvested from the latest FAO (2021), type of water management regime and rice-growing season length from GRiSP (2013), and growth rate of rice area harvested from IFPRI's IMPACT model (2017). Several country-level estimates such as NCCC and NIES and GIR for China, Japan and Korea respectively were also selected as estimates for each country in East Asia.

N_2O emission from agricultural soils associated with fertilizer, crop residues, and other N additions to soils are captured. Both direct and indirect agricultural soil emissions need to be considered. It is primarily (more than half) attributable to the increase of fertilizer input to uplands (Ito et al., 2018). Here we calculated this flux based on a common approach, outlined by Bouwman (1996), in which direct soil N_2O emissions are calculated as the sum of emissions caused by anthropogenic fertilizer-induced emissions plus the remaining background emissions, and the indirect emissions from N volatilization/deposition and N leaching. Data for East Asia was obtained as the ensemble mean of N_2O emissions from national inventories (NCCC, NIES and GIR), some global datasets (the latest CEDS, EDGAR, FAOSTAT, PRIMAP-HIST, EPA), a research study by Cui et al. (2022), and six available model results from NMIP were used for the comparative purpose. Different from using the IPCC Tier 1 methodology as most of the global inventories, Cui et al. (2022) provided a Tier 3 estimate using a linear mixed-effect model and survey-based data set of agricultural management measures to quantify the spatiotemporal changes of crop-specific cropland-N_2O emissions from China between 1980 and 2017.

Aquaculture (Faqua): Aquaculture systems might be potential hotspots for GHG emissions because they have higher biological density and enrichment from fertilizer and feed compared with natural aquatic ecosystems. China is the largest aquaculture producer globally, so errors from omitting in other East Asia countries are expected to be small. In this study, we focused on the emissions from aquaculture in China due to data limitations.

The CH_4 fluxes from aquaculture was acquired from two latest comprehensive studies (Dong et al., 2023; Zhang, Tang, et al., 2022). Zhang, Tang, et al. (2022) presented a nationwide metadata analysis from 132 aquaculture sites in China based on 62 published papers. Four land-based aquaculture systems were considered, including the coastal wetland reclamation system (CWRS), inland pond system (IPS), lake/reservoir system (LRS) and rice-field system (RFS). Dong et al. (2023) analyzed the CH_4 emissions from aquaculture ponds in China with a database of 55 field observations, which corresponds to the emissions from IPS ecosystems.

East Asia contributed 71%–79% of global aquaculture N_2O emissions (Tian et al., 2020). The N_2O emissions were estimated from three different methods for the past 20 years (Hu et al., 2012; Tian et al., 2020; Zhou et al., 2021). Hu et al. (2012) summarized the nitrogen transformation mechanisms of N_2O production and suggested the average N_2O emission factor of aquaculture system is 1.69 g N_2O–N/kg fish globally. We made a rough Tier 1 estimate for East Asia based on this default emission factor by multiplying it with aquaculture production data from FAOSTAT (2022). Using a Tier 2 methodology, Zhou et al. (2021) quantified N_2O emission from Chinese aquaculture systems since the Reform and Opening-up (1979–2019) at the species-, provincial-, and national-levels using annual aquaculture production data, based on nitrogen (N) levels in feed type, feed amount, feed conversion ratio, and emission factors. Tian et al. (2020) provided a comprehensive estimate for the period 2007–2016 with their meta estimate and a nutrient budget model estimate. For Japan, the high consumption of fish is a feature of the Japanese diet (Oita et al., 2018). Hayashi et al. (2021) noticed a high nitrogen use efficiency (NUE) is obtained by fish production due to wild-catch fish, and they estimated the N_2O emission of fish farming area in Japan from 2000 to 2015 to be 0.16 $\sim$ 0.31 Gg N_2O yr^{-1} by using the fate factors of surplus N as 1.25%.

2.4.2.2. Other Sectors

Wetlands methane emission (Fwetland): CH_4 emissions from wetland in this study were mainly derived from the Global Methane Budget (GMB) (Saunois et al., 2020). The GMB provides estimates for East Asia from 13 process-based models during 2000–2017. The dataset WetCHARTs (Bloom et al., 2017) provides global monthly wetland CH_4 emissions and uncertainty from an ensemble of multiple terrestrial biosphere models. However, because the wetland extent simulated by under WetCHARTs protocol differ too large from the satellite-based dataset and each other, we did not use WetCHARTs for budget assessment.

Inland waters outgassing (Fwater): We synthesized CH_4 and N_2O emissions from three types of inland water bodies (includes rivers, natural lakes, reservoirs, lakes regulated by dams) in East Asia. Because the accessible estimates are mostly static or with short temporal coverage, we assumed no interannual variations for Fwater during 2000–2019. For CO_2 we obtained estimates from 10 studies, while for CH_4 and N_2O, we obtained from eight studies and five studies, respectively.

Fire CH_4 and N_2O emissions (Ffire): Similar to the CO_2 emissions from fires, we used GFEDv4.1s (van der Werf et al., 2017) to estimate CH_4 and N_2O emissions in this sector. Emissions of five different fire types were considered.

Natural soil CH_4 sink and N_2O source (Fnatusoil): Oxidation of atmospheric CH_4 by methanotrophs in natural soils and N_2O emissions from unmanaged soil were evaluated by the process-based terrestrial ecosystem model VISIT (Ito, 2021; Ito et al., 2018), which contained four schemes for simulating the process. Results from simulating natural vegetation and croplands separately at each grid were used. The output data was at $0.5° \times 0.5°$ resolution and a timeseries between 2000 and 2016 was extracted for our estimation.

Termites CH_4 emission (Ftermite): Termites are a CH_4 source (Ito et al., 2019), which is related to symbiotic cellulose-digesting microbes in their digestive tracts. Given the difficulty in mapping the regional distribution of termites, our estimate was simply based on the conventional empirical estimation after Ito et al. (2019) who used land-use data and emission factors from the literature.

2.5. Calculation of Net GHG Budgets

We then tried to make top-down and bottom-up results comparable through lateral flux adjustments for each greenhouse gas following the formula below:

$$\mathrm{TD}_{\mathrm{CO_2}} = \text{inversion } \mathrm{CO_2} \text{ flux} + F_{\mathrm{frcc}} + F_{\mathrm{brcc}} + F_{\mathrm{trade}} \quad (1)$$

$$\mathrm{TD}_{\mathrm{CH_4}}{}^{a} = \text{inversion } \mathrm{CH_4} \text{ total flux} - F_{\mathrm{fossil}}{}^{b} - F_{\mathrm{waste}}{}^{c} - F_{\mathrm{geology}}{}^{d} \quad (2)$$

$$\mathrm{TD}_{\mathrm{N_2O}} = \text{inversion } \mathrm{N_2O} \text{ flux} - F_{\mathrm{fossil}} - F_{\mathrm{waste}} \quad (3)$$

$$\mathrm{BU}_{\mathrm{CO_2}} = \Delta\mathrm{C}_{\mathrm{forest}} + \Delta\mathrm{C}_{\mathrm{grassland}} + \Delta\mathrm{C}_{\mathrm{cropland}} + \Delta\mathrm{C}_{\mathrm{other}} + \Delta\mathrm{C}_{\mathrm{burial}} + \Delta\mathrm{C}_{\mathrm{product}} + F_{\mathrm{export}} \quad (4)$$

$$\mathrm{BU}_{\mathrm{CH_4}} = F_{\mathrm{enteric}} + F_{\mathrm{manure}} + F_{\mathrm{agrisoil}} + F_{\mathrm{aqua}} + F_{\mathrm{wetland}} + F_{\mathrm{natusoil}} + F_{\mathrm{fire}} + F_{\mathrm{water}} + F_{\mathrm{termite}} \quad (5)$$

$$\mathrm{BU}_{\mathrm{N_2O}} = F_{\mathrm{manure}} + F_{\mathrm{agrisoil}} + F_{\mathrm{aqua}} + F_{\mathrm{natusoil}} + F_{\mathrm{fire}} + F_{\mathrm{water}} \quad (6)$$

Note: [a]Top-down budget: the fossil fuel emission is assumed well known by CO_2 inversions. [b]Ffossil: fossil fuel induced GHG emissions. [c]Fwaste&landfill: waste treatments and landfills induced emissions (data reference: CEDS, EDGAR, IIASA GAINS and PRIMAP). [d]Fgeology: geological seepage induced CH_4 emissions (data reference: Etiope et al., 2019).

The total influence of three greenhouse gases was calculated separately for bottom-up and top-down approaches. GWP100 and GWP20 (global warming potentials on 100-year or 20-year time horizon) were used to estimate the integrated radiative forcing of CH_4 and N_2O in terms of a CO_2 equivalent unit. We adopt 100-year GWPs of 27.0 and 273 for CH_4 and N2O, 20-year GWPs of 79.7 and 273 for CH_4 and N_2O, respectively, according to IPCC AR6 WG1Table 7.15 (Canadell et al., 2021; IPCC, 2022). The GHG budget is therefore combining the three main GHG gases with the following equation (Figure 4):

$$\mathrm{GHG} = \mathrm{Budget}(CO_2) + \mathrm{Budget}(CH_4) * GWP_{CH_4} + \mathrm{Budget}(N_2O) * \mathrm{GWP}_{N_2O} \ (\mathrm{unit}: CO_2\mathrm{eq}) \quad (7)$$

2.6. Uncertainty Estimates

Uncertainty in the total budget for each greenhouse gas was obtained by error propagation from uncertainties of each term from Equation 1 to Equation 6, assuming each flux term is independent to each other. The standard deviation of different estimates over the past 20 years was calculated at the national scale as the uncertainty for the flux term. As for few flux terms which only have one available estimate, the reported uncertainty for the estimate by the original paper was considered as the uncertainty of this term. Further details in uncertainty reports (Text S10 in Supporting Information S1) and robustness tests (Text S11, Figure S7 in Supporting Information S1) can be found in Supporting Information S1.

3. Results and Discussions

3.1. CO_2 Budget

3.1.1. Top-Down

An ensemble of seven atmospheric inversion models and three inversions using additional regional observations estimated East Asia to have a net land-to-atmospheric CO_2 flux of -1516.6 ± 419.5 Tg CO_2 yr^{-1} (Table 1), ranging from -662.5 Tg CO_2 yr^{-1} to -1770.5 Tg CO_2 yr^{-1}. According to the seven global atmospheric inversions, this accounts for 18% of global land CO_2 sink. We adopted three regional inversions (Chen et al., 2021; Jiang et al., 2016; Y. Wang et al., 2022), which used latest available CO_2 measurements by Chinese Meteorological Administration not included in the global inversions. These regional inversions did not show significant differences with the global inversions for East Asia's land CO_2 sink. By adjusting for the CO_2 fluxes induced by lateral C transport processes (net trade of food and wood products, reduced carbon compounds of fossil fuel and biogenic sources) (Ciais et al., 2019; Y. Wang et al., 2022), the terrestrial ecosystem over East Asia is a net sink of CO_2 by -1229.3 ± 430.9 Tg CO_2 yr^{-1}.

3.1.2. Bottom-Up

Forests expanded rapidly during the study period over East Asia. According to FAO, forest area increased by more than 15% from 2.3×10^8 ha in 2000 to 2.7×10^8 ha in 2020, accounting for ~7% of global forests. Adding up forest inventory estimates from East Asian countries, the carbon stock in East Asia's forest increased by 788.6 ± 142.2 Tg CO_2 yr^{-1}, which is mostly contributed by forest plantation in China (Yu et al., 2022). The forest carbon sink was largely due to increasing biomass, which was reported consistently by ground forest surveys and passive microwave measurements (see Methods). Shrublands, grasslands, croplands and wetlands were also found to be weaker CO_2 sinks of -126.3 ± 42.2 Tg CO_2 yr^{-1}, -36.4 ± 45.2 Tg CO_2 yr^{-1}, -66.3 ± 15.4 Tg CO_2 yr^{-1}, -44.7 ± 0.4 Tg CO_2 yr^{-1}, respectively (Table 1). Adding up the carbon burial in inland waters and the accumulated carbon in wood products (see Methods), the inventory-based method estimated an East Asia's CO_2 sink of -1353.8 ± 158.5 Tg CO_2 yr^{-1}.

3.1.3. CO_2 Budget Synthesis

It is encouraging to see the top-down and bottom-up estimates of land CO_2 sink are within ±10% of one another (between -1229.3 ± 430.9 Tg CO_2 yr^{-1} and -1353.8 ± 158.5 Tg CO_2 yr^{-1}) during 2000s and 2010s, though both estimates were larger than the ensemble mean of Net Biome Production estimated by the 18 TRENDY ecosystem models (-978.9 ± 316.8 Tg CO_2 yr^{-1}) (Friedlingstein et al., 2022). Although smaller-scale spatial variations within the region exist between 18 TRENDY models (Figure S2 in Supporting Information S1), all the models agree that China contributed the most (about 80%~90%) to the carbon sink in East Asia, followed by Japan, Koreas and Mongolia (Figure S1 in Supporting Information S1). It should be noted that these TRENDY model estimates were forced by varying climate and CO_2, but by constant land cover. There is emerging evidence from forest inventories, remote sensing and process-based and book-keeping models that land cover and land use change flux (Fluc) in East Asia is a strong net sink of atmospheric CO_2 (e.g., Piao et al., 2018; Yu et al., 2022, Leng et al. under review). Based on our synthesis, we estimated that Fluc over East Asia as a sink of -290.2 Tg CO_2 yr^{-1}. Adding TRENDY model NEE and this Fluc, the resulting land CO_2 sink estimate was -1269.1 ± 423.9 Tg CO_2 yr^{-1}, close to both the top-down and bottom-up estimates.

Table 1
The GHG Budget in East Asia Since 2000

Sectors		CO_2 (Tg CO_2 yr^{-1})		CH_4 (Tg CH_4 yr^{-1})		N_2O (Tg N_2O yr^{-1})	
		Mean	Uncertainty[a]	Mean	Uncertainty	Mean	Uncertainty
1. Human activities	1.A Fossil Fuel	9493.35	221.83	23.40	1.90	0.58	0.05
	1.B Waste and Landfill			11.38	3.20	0.32	0.48
	Subtotal	**9493.35**	**221.83**	**34.79**	**3.72**	**0.90**	**0.49**
2. Carbon stock change	2.A Forests	−788.55	142.22	–	–	–	–
	2.B Shrublands	−126.25	42.21	–	–	–	–
	2.C Grasslands	−36.37	45.24	–	–	–	–
	2.D Croplands	−66.27	15.44	–	–	–	–
	2.E Wetlands	−44.66	0.40[b]	–	–	–	–
	2.F Urban Construction	1.62	0.83	–	–	–	–
	2.G Burial	−37.79	24.24	–	–	–	–
	2.H Wood Products	−103.07	10.46	–	–	–	–
	Subtotal	**−1201.33**	**158.09**	–	–	–	–
	NEE	−978.94	316.76	–	–	–	–
	Land Cover and Land Use Change	−290.17	281.72	–	–	–	–
	Subtotal	**−1269.10**	**423.92**	–	–	–	–
3. Lateral adjustments	3.A Net Trade	−171.11	70.75	–	–	–	–
	3.B Lateral Transport to Ocean	−152.48	11.68	–	–	–	–
	3.C Fossil Fuel RCC	322.67	18.33	–	–	–	–
	3.D Biogenic RCC	135.67	66.00	–	–	–	–
4. Agriculture	4.A Enteric Fermentation	–	–	9.60	1.34		
	4.B Manure Management	–	–	1.91	0.92	0.30	0.11
	4.C Agricultural Soil	–	–	9.26	2.82	0.80	0.26
	4.D Aquaculture	54.93	21.00	2.27	0.94	0.07	0.05
	Subtotal	–	–	**23.04**	**3.37**	**1.17**	**0.29**
5. Other sectors	5.A Wetlands	–	–	3.46	0.50		
	5.B Natural Soil	–	–	−2.62	0.26	0.78	0.09
	5.C Fires	84.36	12.56	0.28	0.03	0.01	0.00
	5.D Inland Waters	348.40	146.66	4.09	1.77	0.04	0.03
	5.E Termites	–	–	0.32			
	Subtotal	–	–	**5.53**	**1.86**	**0.83**	**0.09**
	5.H Geological Seepage[c]	–	–	2.17	0.43	–	–
	TD Inversion	−1516.55	419.46	30.30	5.17	1.34	0.83
Balance	**BU Land Budget**	**−1353.81**	**158.52**	**28.57**	**3.85**	**2.00**	**0.31**
	TD Land Budget	**−1229.33**	**430.86**	**30.30**	**5.17**	**1.34**	**0.83**

Note. Bold values represent the subtotal of each sector or the total budget of each GHG. [a]The reported uncertainty represents the standard deviation. [b]The uncertainty for 2.E is estimated as 21% of the mean value (NCCC, 2018). [c]Geological seepage is not contained within the boundaries of our terrestrial ecosystem framework.

We also noted that uncertainties associated with Fluc remain large for East Asia. When forced with varying land cover, all TRENDY models estimated Fluc over East Asia as a net source of CO_2 of more than 100 Tg C yr^{-1} (Figure 3), especially in China (Figure S3 in Supporting Information S1). The spatial patterns of Fluc varied greatly among TRENDY models (Figure S4 in Supporting Information S1), which implies that in East Asia, the performance of carbon cycle model-based inference of Fluc still need to be improved. Such issue also occurred in estimates from Hansis et al. (2015). This is probably because both TRENDY models and Hansis et al. (2015) were driven by a common land use forcing LUH2 (Chini et al., 2021) which reported increasing cropland area and

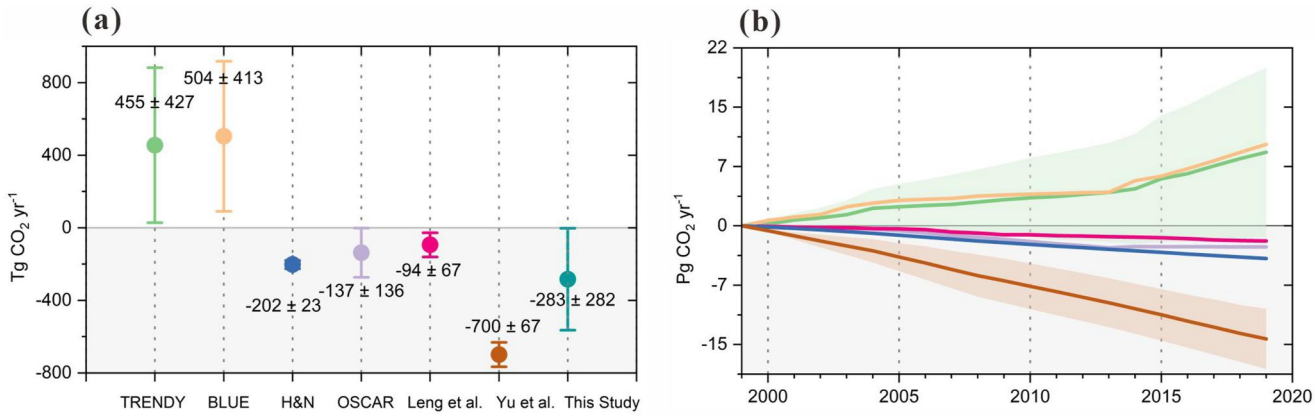

Figure 3. Comparison of different estimates on flux of land cover and land use change (Fluc) in East Asia. (a) Different Fluc estimates over East Asia; (b) Cumulative Fluc over EA from 2000 to 2019.

decreasing forest area over East Asia. This contradicts the evidence from ground and satellite observations (e.g., Piao et al., 2018; Yu et al., 2022, Leng et al. under review).

The land CO_2 sink over East Asia contributes more than one sixth of the global land CO_2 sink (Friedlingstein et al., 2022), which means its CO_2 sink per area is stronger than the global average. However, the sink offsets fossil fuel emissions of East Asia by less than 15% (Friedlingstein et al., 2022). It implies that even tripling the land CO_2 sink over East Asia, will still not satisfy carbon neutrality ambitions of East Asian countries. Thus, a realistic pathway of carbon neutrality would have to combine both CO_2 emission reduction and CO_2 sink enhancement.

3.2. CH_4 Budget

3.2.1. Top-Down

There are 10 atmospheric inversion models for estimating CH_4 fluxes over East Asia, which yielded the CH_4 emission from terrestrial ecosystems as 30.3 ± 5.2 Tg CH_4 yr^{-1} (Table 1) for the decades of 2000s and 2010s, after adjusting for fossil fuel, waste and landfill emissions and geological seepage (see Methods). The global CH_4 inversion models provided by GCP (Saunois et al., 2020) basically used the same set of observations reporting on the range from 25.7 Tg CH_4 yr^{-1} to 40.4 Tg CH_4 yr^{-1}, while the regional inversion by Zhang, Fang, et al. (2022) using seven additional sites over China reported 31.2 Tg CH_4 yr^{-1} which is also within the range of the global inversions. These results were also consistent with Thompson et al. (2015), whose inversion used CH_4 and its isotope measurements with a nested grid over East Asia.

3.2.2. Bottom-Up

The CH_4 fluxes can be broadly classified into two sectors (Figure 2), the agricultural sector (enteric fermentation, manure management, paddy croplands and freshwater aquaculture) and the natural ecosystem sector (wetlands, lake, ponds and other inland water bodies, wild fires, termites, and soil uptake). Spatial pattern of bottom-up CH_4 budget in available sector is shown in Figure S5 in Supporting Information S1.

For the agricultural sector, the largest flux term was found to be the enteric fermentation by ruminant animals (9.6 ± 1.3 Tg CH_4 yr^{-1}). Although traditional meat sources of East Asian countries are swine and poultries (chickens and ducks), there is a growing consumption of beef and lamb. If such tendency persists, the local production could become the dominant source of CH_4 emission in this region, though the per capita consumption of beef and lamb over East Asia are still below the global average (FAO, 2022). One of the collateral consequences of both ruminant animals and swine and chickens is CH_4 emission from manure management, which amounts to 1.9 ± 0.9 Tg CH_4 yr^{-1}. Another large flux term is CH_4 emission from paddy rice fields (9.3 ± 2.8 Tg CH_4 yr^{-1}). Since rice is the primary staple food for China, Japan, South Korea and North Korea, East Asia contains ~20% of global rice croplands (Figure 1), the majority of which is flooded and more productive than the

global average. Thus, it is not surprising that about one third of the global CH_4 emission in paddy rice fields comes from the East Asia region (Saunois et al., 2020). Another smaller but significant flux is CH_4 emission from freshwater aquaculture (2.3 ± 0.9 Tg CH_4 yr^{-1}), because more than 60% of the global freshwater aquaculture products comes from East Asia, in particular China (FAO, 2021; Yuan et al., 2019; Zhou et al., 2021). Overall, the agricultural sector emits 23.0 ± 3.4 Tg CH_4 yr^{-1} (Table 1).

For natural ecosystems, the largest sources were wetlands and inland water bodies (lakes, ponds and reservoirs), which we estimated as 3.5 ± 0.5 Tg CH_4 yr^{-1} and 4.1 ± 1.8 Tg CH_4 yr^{-1}, respectively, according to several global and regional studies (see Methods). The ensemble of 13 wetland models estimated a broad range of CH_4 emission from 0.8 ± 0.2 to 10.4 ± 0.5 Tg CH_4 yr^{-1}. The wetland CH_4 emission over East Asia only contributes less than 2% of global wetland CH_4 emission (Saunois et al., 2020), partly because the small fraction of global wetland area (~4%), according to global dataset of Wetland Area and Dynamics for Methane Modeling (WAD2M; Zhang, Fluet-Chouinard, et al. (2021)). The sink of CH_4 by non-saturated oxygenated soil is the primary land sink, which was estimated as -2.6 ± 0.3 Tg CH_4 yr^{-1} over East Asia, whose global contribution is commeasurable to its land fraction. CH_4 emissions from wild fires (0.3 ± 0.1 Tg CH_4 yr^{-1}) and termites (~0.3 Tg CH_4 yr^{-1}) were relatively small over East Asia. All added together, natural ecosystems emit 5.5 ± 1.9 Tg CH_4 yr^{-1} (Table 1).

3.2.3. CH_4 Budget Synthesis

It appears encouraging to find the bottom-up estimates of land CH_4 emission over East Asia (28.6 ± 3.9 Tg CH_4 yr^{-1}) to be close (about ±5%) to the top-down estimates of the land CH_4 emission (30.3 ± 5.2 Tg CH_4 yr^{-1}). However, this could be in part coincident given the large uncertainties in some major flux terms, as the variation within BU ensembles and within TD ensembles is larger than their difference. For example, the challenge to estimate CH_4 ebullition from inland waters remain a major source of uncertainties for inland water CH_4 emissions that studies may differ by one order of magnitude (e.g., Chen et al., 2013; Stavert et al., 2021). The agricultural sector is the dominant sources of land CH_4 emission, whose magnitudes was three times more than the CH_4 emissions from natural ecosystems. The high intensity of rice cultivation and inland water aquaculture has made East Asia's contribution to global land CH_4 emission larger than its land fraction (~8%). Unlike CO2, the magnitude of anthropogenic CH4 emissions from fossil fuel combustion and waste and landfill has a similar magnitude (34.8 ± 3.7 Tg CH_4 yr^{-1}) to land CH4 emissions at the same period (Table 1).

3.3. N_2O Budget

3.3.1. Top-Down

The four atmospheric inversion models reported an average estimate of land N_2O emissions over East Asia of 1.3 ± 0.8 Tg N_2O yr^{-1} during 2000s and 2010s, with individual estimates ranging from 0.5 Tg N_2O yr^{-1} to 2.2 Tg N_2O yr^{-1}. Compared with CO_2 and CH_4, the available N_2O observation sites remain scarce globally (Thompson et al., 2019), and only few sites were distributed in or around East Asia. Therefore, the smaller relative uncertainties among the N_2O inversion models should be treated with caution, since the estimates were poorly constrained by regional observations, and the uncertainties associated with different sets of observations were not considered in this model ensemble. For similar reasons, the hotspots of the N_2O emissions should come mostly from the prior flux pattern (Figure 5), rather than observational constraints.

3.3.2. Bottom-Up

The land N_2O emissions could also be classified into two general categories (Figure 2), the agricultural sector (manure management, cropland, and freshwater aquaculture) and the natural ecosystem sector (natural soils, wild fires, and inland water bodies).

The cropland N_2O emission was found to be the largest flux at 0.8 ± 0.3 Tg N_2O yr^{-1}(Table 1). It contributes to about one fifth of global cropland N_2O emission (Wang et al., 2020), which is due to the excessive nitrogen fertilizer input in some East Asian countries (e.g., Yu, Huang, et al., 2019). We estimated the second largest emission source to be from manure management (0.3 ± 0.1 Tg N_2O yr^{-1}), with individual estimates by inventories or process-based models differing by five times from 0.1 Tg N_2O yr^{-1} to 0.5 Tg N_2O yr^{-1} (see Methods). The lack of spatially explicit data of storage duration and treatment type for livestock dung and urine could be responsible for the large uncertainties, as well as the potential biases of the fraction of total nitrogen

excretion by livestock species/categories and manure management system and the associated emission factors (Cui et al., 2021). The freshwater aquaculture is also a non-negligible N_2O emission source (0.1 ± 0.1 Tg N_2O yr^{-1}), given much more intense nitrogen input into these fish/shrimp/crab farms than the other inland water bodies and its wide distribution over East Asia, in particular over China (Yuan et al., 2019). Because N_2O emission estimates for freshwater aquaculture were mostly available over China, we had to use all available Chinese estimates and only one available Japanese estimate to represent the East Asia. This should lead to a minor underestimate given the small ratio (<5%; FAO, 2022) of contributions of other countries to the East Asian freshwater aquaculture production.

On the natural sector, natural soil emission was found to be the predominant source (0.8 ± 0.1 Tg N_2O yr^{-1}), according to the VISIT model (Ito et al., 2018). Apparently, although nitrogen deposition over East Asia is much higher than the global average (e.g., Yu, Jia, et al., 2019), its contribution to global natural soil N_2O emission (Tian et al., 2020) is sizable to or even smaller than East Asian land fraction due to large dryland area in its western part. The sum of wild fires and inland water N_2O emissions were less than 0.1 Tg N_2O yr^{-1} (Table 1), resulting in a synthesized natural sector N_2O emission estimate of 0.8 ± 0.1 Tg N_2O yr^{-1}.

3.3.3. N_2O Budget Synthesis

Overall, we found the bottom-up estimate of land N_2O emissions over East Asia was 2.0 ± 0.3 Tg N_2O yr^{-1}, while the top-down estimate was 1.3 ± 0.8 Tg N_2O yr^{-1}. This regional source of N_2O contributes to more than 30% of global land N_2O emission (Tian et al., 2020), highlighting East Asia as the global hotspot region for curbing N_2O emissions. Among the flux terms, the agricultural sector accounted for more than 60% of all N_2O emissions, despite the fact that croplands only occupy less than 20% of the land area. The land N_2O emissions over East Asia was two times than the anthropogenic N2O emission from fossil fuel combustion and waste and landfill (9.0 ± 0.5 Tg N_2O yr^{-1}) for the same period (Table 1). Compared with CO_2 and CH_4, the consistency of N_2O emission between the top-down and bottom-up estimates were the poorest (>30%), reflecting the larger uncertainties in assessing the more potent greenhouse gas, both for the top-down and for the bottom-up estimates. Unlike CO_2 and CH_4, there is no direct satellite N_2O measurements to be used for atmospheric inversion (Shen et al. in review). Considering also the fewest available measurement sites, there is an urgent need for increasing the number of N_2O observation sites. In addition, the inventory-based estimates also vary by 3–5 times at country/regional scales, highlighting the need to further develop spatial representation of agricultural management practices (e.g., fertilization, irrigation, tillage, manure storage, and treatment) and the emission factors, which would also support the development of mitigation strategies to address nitrogen pollution in air and waters (e.g., Gu et al., 2023).

3.4. Greenhouse Gas Synthesis

We used greenhouse gas warming potential (GWP) on the 100-year time horizon (IPCC, 2021; Table S4 in Supporting Information S1) to account for varying impacts of the three greenhouse gases in our assessment on the overall GHG gas balance of the region and thus reflecting its impacts on the global climate system. The net source of CH_4 was estimated at 818.0 ± 139.6 Tg CO_2eq yr^{-1} by the top-down approach and at 771.3 ± 104.0 Tg CO_2eq yr^{-1} by the bottom-up approach. The net source of N_2O was estimated as 365.1 ± 225.3 Tg CO_2eq yr^{-1} by the top-down approach and 546.1 ± 83.4 Tg CO_2eq yr^{-1} by the bottom-up approach. In either approach, the net sink of CO_2 (−1229.3 ± 430.9 Tg CO_2 yr^{-1} by the top-down and −1353.8 ± 158.5 Tg CO_2 yr^{-1}) exceeded the net sources of CH4 and N_2O, rendering the land over East Asia is nearly GHG neutral (−46.3 ± 505.9 Tg CO_2eq yr^{-1} by the top-down and −36.1 ± 207.1 Tg CO_2eq yr^{-1} by the bottom-up) (Figure 4; Table 2). GHG balance based on GWP on the 20-year time horizon was also calculated (Table 2), the overall source is substantially stronger due to the much higher weight of short-lived CH4, emphasizing the challenge of developing sustainable technical approaches to reduce CH4 emissions without compromising the agricultural demand. No matter for the 100-year or 20-year horizon, the climate mitigation effects of the CO_2 uptake by terrestrial ecosystems in the East Asia region could have been largely canceled out (>90%; Table 2) by its net release of CH_4 and N_2O into the atmosphere.

When we separated the land ecosystems into agricultural ecosystems and natural ecosystems, which was only possible in bottom-up approach, we found that the natural ecosystems over East Asia were a significant net GHG sink (−911.5 ± 167.4 Tg CO_2eq yr^{-1}), which was offset by the net GHG source of agricultural ecosystems (875.4 ± 121.9 Tg CO_2eq yr^{-1}). This was also consistent with the location of hotspots of CH_4 and N_2O

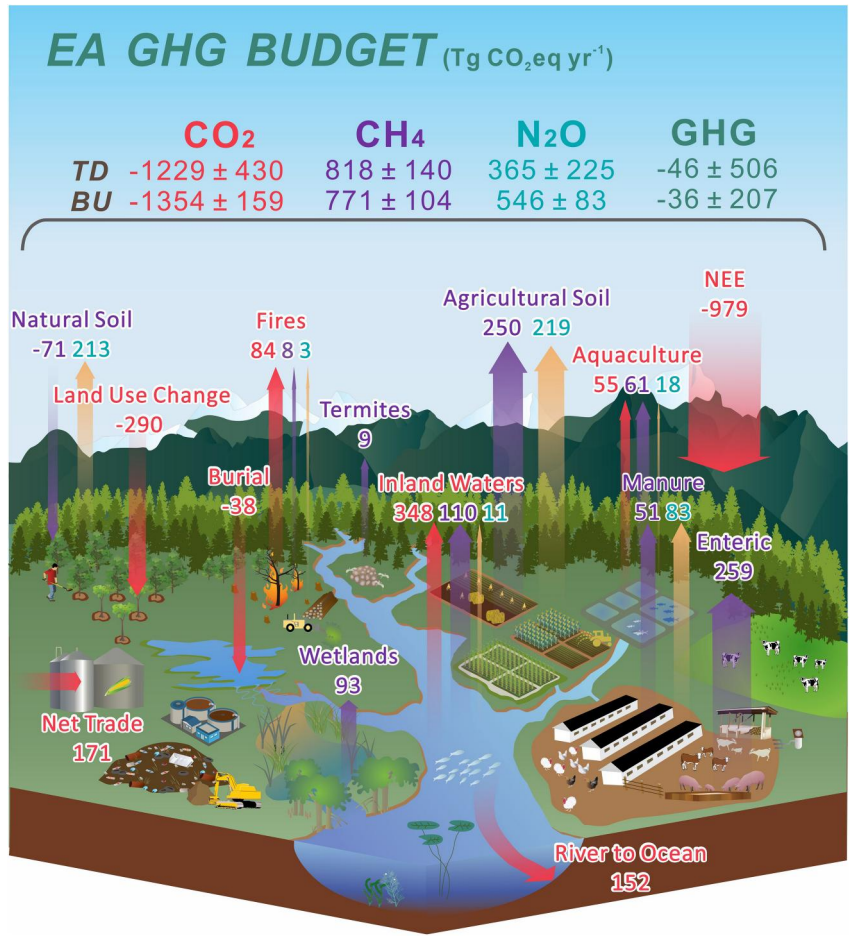

Figure 4. East Asia greenhouse gas (GHG) budget during 2000s and 2010s. The color arrows represent GHG fluxes (in Tg CO_2eq yr^{-1} for 2000–2019) as follows: red, CO_2; purple, CH_4; blue, N_2O. Definitions and explanations of the flux terms can be found in the Methods section.

Table 2
Terrestrial GHG Budget Based on GWP100 and GWP20 Metrics

	CO_2		CH_4		N_2O		GHG total			
Terrestrial GHG budget (Tg CO_{2eq} yr^{-1})	Mean	sd	Mean	sd	Mean	sd	Mean	sd	P1[a]	P2[b]
GWP100										
TD	−1229.3	430.9	818.0	139.6	365.1	225.3	−46.3	505.9	96%	836%
BU	−1353.8	158.5	771.3	104.0	546.4	83.4	−36.1	207.1	97%	760%
Natural	−1287.5	157.8	149.3	50.1	226.7	25.3	−911.5	167.4	29%	–
Agricultural	−66.3	15.4	622.0	91.1	319.7	79.5	875.4	121.9	1421%	–
GWP20										
TD	−1229.3	430.9	2414.6	412.2	365.1	225.3	1550.3	637.4	226%	937%
BU	−1353.8	158.5	2276.7	306.9	546.4	83.4	1469.3	355.3	209%	851%
Natural	−1287.5	157.8	440.8	147.9	226.7	25.3	−620.0	217.7	52%	–
Agricultural	−66.3	15.4	1835.9	268.9	319.7	79.5	2089.4	280.8	3,253%	–

[a]Proportion of land CO_2 sink being offset by terrestrial GHG source. [b]Proportion of land CO_2 sink being offset by total fossil fuel source.

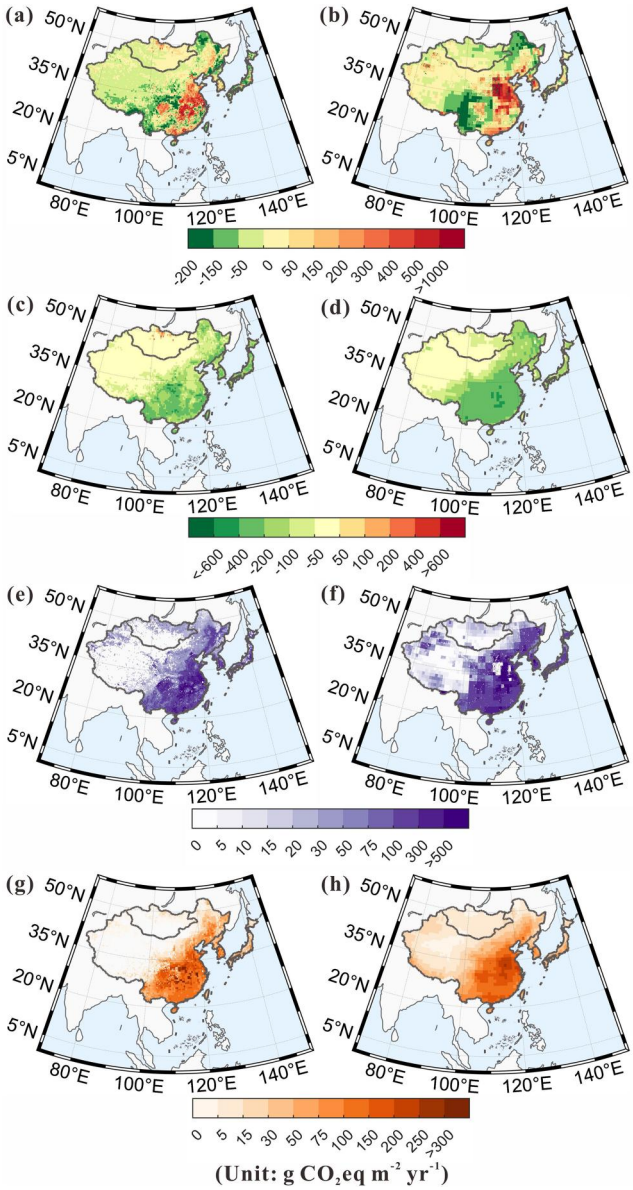

Figure 5. Spatial pattern of greenhouse gas (GHG) balance. (a) GHG balance estimated by the bottom-up approach; (b) GHG balance estimated by the top-down approach; (c) Net Biome Production simulated by dynamic global vegetation models; (d) CO_2 balance estimated by the atmospheric inversions; (e) CH_4 balance estimated by the inventory-based approach; (f) CH_4 balance estimated by the atmospheric inversions; (g) N_2O emission estimated by the inventory-based approach; (h) N_2O budget balance estimated by the atmospheric inversions (unit: g CO_2eq m^{-2} yr^{-1}).

emissions, and thus net GHG emission, over areas dominated by cropland, such as the North China Plain (the region's wheat basket with widespread wheat-maize rotated croplands) and southern China (rice cultivated for two or three seasons) (Figure 5). These results highlighted that the agricultural sector as the priority for climate change mitigation in terrestrial ecosystems.

An in-depth discussion on the effect of estimates from global datasets (e.g., bottom-up estimates from global inventories, GCB, FAO, EDGAR) and regional datasets with additional regional information (e.g., national and regional inventories using regional specific emission factors and activity data, inversion estimates with additional regional observational sites) has been made. The results showed that all terms were within the reported uncertainty range of two sources of datasets (Table S5 in Supporting Information S1). While the estimates of some terms (e.g., Fluc, Ftrade and Fmanure) showed quite different, suggesting more efforts should be made to recognize their characteristics regionally, for which we have carefully analyzed and discussed. It should be noted that estimates of non-CO_2 GHG fluxes from natural sources have been relatively poorly constrained in regional scale, which require future studies to quantify the emissions from the natural sectors.

In summary, using either global data streams or regional data streams result in no significant change to the main conclusions of this study (Tables S5 and S6 in Supporting Information S1). It is not yet mature to claim whether one type is better than the other based on their spatial coverage. We utilized both types of data streams in our synthesis, hoping to maximize the community wisdom as suggested by the RECCAP methodology (Canadell et al., 2011).

Among the three GHGs, CO_2 fluxes were largest in the magnitude and uncertainties (Figure 6 and Figure S6 in Supporting Information S1). Compared with the RECCAP-1, which demonstrated that terrestrial ecosystem over East Asia was a net CO_2 sink between -806.7 Tg CO_2 yr^{-1} (bottom-up) and -990.0 Tg CO_2 yr^{-1} (top-down) during 1990s and 2000s (Piao et al., 2012), the new estimates on East Asia's CO_2 sink appear more convergent between the bottom-up and the top-down approaches, with differences within ±10%. However, large uncertainties remain in several flux terms. For example, forest CO_2 sink contributes to more than half of the land CO_2 sink and ~75% of the uncertainties in land CO_2 sink, despite new sources of independent data emerging recently, such as forest biomass estimates from both passive satellite microwave measurements (e.g., Chang et al., 2023) and the combined LIDAR and multi-spectral optical remote sensing (e.g., Xu et al., 2021). Constraining soil carbon budget also needs additional data and efforts. CH_4 emission from the paddy fields and N_2O emission from cropland soils contribute the largest to uncertainties in CH_4 and N_2O emissions, respectively (Figure 6).

3.5. Uncertainty Analysis

To better clarify the uncertainties related to datasets with different spatial and temporal resolutions, we performed sensitivity analysis on the sample size and temporal coverage of data used in this study (Text S11). Results showed that the uncertainty caused by the differences in the temporal coverage is less than 10% of our reported estimates (Figure S8 in Supporting Information S1), implying minor impacts from the temporal coverage differences and the robustness of our estimation during 2000s and 2010s. Furthermore, The analysis also indicates that our estimation should not be sensitive to inter-annual events, which is one of the reasons why RECCAP-2

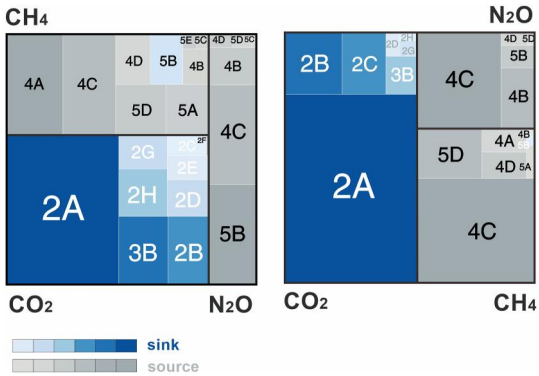

Figure 6. Contribution of major flux terms to the magnitude of greenhouse gas budgets and to the uncertainties based on GWP100. The blue block indicates the GHG sink, the gray block indicates the GHG source. The thick black lines distinguish the three gases. (left) Contribution of each flux term to the magnitude of GHG budgets. (right) Contribution of each flux term to the overall uncertainties.

chose the two decades as the study period, rather than a shorter study period. The uncertainties associated with sample size is minor in our analysis (Figure S9 in Supporting Information S1). The differences in spatial resolution will incur uncertainties for spatial patterns of the GHG budget. However, the main conclusions of this study were drawn from the regional scale aggregated over all East Asian countries. The spatial resolution of the data streams (higher than 0.5° for bottom-up approaches and ~1° for top-down approaches) are in general fine enough for assessing the budget over the entire region, though the robust smaller-scale spatial variations within the region should be explored with additional efforts in the future. We have also noted the cautions needed for the pattern of GHG budget in fine spatial details.

Based on our analysis, we indicated that a robust synthesis of each flux term should contain at least five estimates covering more than 12 years in this study. The spatial resolution of data streams is suggested to be as high as possible. Divergent estimates with contradicted results should be treated with caution. For example, in this study, with the assumption of increasing forest area in China with ground-based and satellite evidence, we excluded estimates of Fluc driven by land use forcing suggesting the increasing cropland area and decreasing forest area in China during the 2000s and 2010s.

4. Conclusions

Terrestrial ecosystems over East Asia were net GHG neutrality based on the dual-constraint of top-down and bottom-up approaches during 2000s and 2010s, indicating that the CO_2 sink in the ecosystems could have been largely offset by the net source of CH_4 and N_2O. Compared to the global GHG estimate from Tian et al. (2016), both of our top-down and bottom-up estimates indicated that CH_4 and N_2O budgets of East Asia account for ~15% of the global budget, while the corresponding proportion of CO_2 sink to the globe is more than 20% (top-down: 21%; bottom-up: 26%). The remarkable carbon sink capacity of East Asia made the overall balance of terrestrial ecosystem GHG close to neutral. While natural ecosystems were a net sink of GHG, it has been almost fully offset by net sources of GHG from the agricultural ecosystems. This study highlights the agricultural sector as a priority for climate mitigation efforts on terrestrial ecosystems over East Asia. The emerging data sources, improving modeling capacities in recent years have contributed to the improved closure between top-down and bottom-up estimates, though sizable uncertainties remain in some major flux terms, such as land use change. Future studies should need to further refine emission factors and activity data to provide estimates with better spatial and temporal resolutions, which would not only facilitate the policy making for climate change mitigation, but also serve monitoring the progresses in achieving climate neutrality.

Data Availability Statement

The relevant data supporting the conclusions of this study, including the inversion fluxes for three GHGs, the GCP estimates for three GHGs, the regional land carbon fluxes of TRENDYv9, the soil N2O emissions estimated by NMIP models, the book-keeping model fluxes, the synthesis of inland water GHG emission estimates and the lateral carbon fluxes were archived and available from the data repository of RECCAP-2 at https://www.bgc-jena.mpg.de/geodb/projects/Home.php. All other datasets used in this study were listed in Table S1–S3 in Supporting Information S1 with detailed data descriptions and link for access. The analysis was conducted through MATLAB version R2022a (https://ww2.mathworks.cn/products/matlab.html). Maps and figures were created through ArcGIS Pro version 2.8.3 from Esri (https://www.esri.com/en-us/arcgis/products/arcgis-pro/overview) and CorelDraw Graphics Suite version 2021 from Corel Corporation (https://www.coreldraw.com/en/product/coreldraw/). Any other request should be directed to the corresponding author.

Acknowledgments
This study was supported by National Natural Science Foundation of China (No. 42171096 & 42041007) and Ministry of Science and Technology of People's Republic of China (No. 2019YFA0607302). Ronny Lauerwald acknowledges funding from French state aid, managed by ANR under the "Investissements d'avenir" programme (ANR-16-CONV-0003). The updated CO_2 and CH_4 inversions using MIROC4-ACTM are prepared by Naveen Chandra and Dmitry Belikov, respectively. Patra Prabir is partly supported by the Arctic Challenge for Sustainability phase II (ArCS-II; JPMXD1420318865) and Environment Research and Technology Development Fund (SII8; JPMEERF21S20800), Government of Japan. Net CO_2 flux estimates from the University of Edinburgh are provided by Liang Feng and Paul Palmer who acknowledge funding from the UK National Centre for Earth Observation (NE/R016518/1). We thank Dr. Ingrid Luijkx for providing atmospheric CO_2 inversions and suggestions to the manuscript. The PyVAR-CAMS modeling results were funded through the Copernicus Atmosphere Monitoring Service implemented by ECMWF on behalf of the European Commission, and were generated using computing resources from LSCE.

References

Allen, G. H., & Pavelsky, T. M. (2018). Global extent of rivers and streams. *Science*, *361*(6402), 585–588. https://doi.org/10.1126/science.aat0636
Arjo, S., Janot, T., & Sander, H. (2020). Description of the CH4 inversion production chain 2020 (CAMS73_2018SC3_D73.5.2.2-2020_202012_production_chain_v1).

Bastos, A., Ciais, P., Sitch, S., Aragão, L. E. O. C., Chevallier, F., Fawcett, D., et al. (2022). On the use of Earth observation to support estimates of national greenhouse gas emissions and sinks for the global stocktake process: Lessons learned from ESA-CCI RECCAP2. *Carbon Balance and Management*, *17*(1), 15. https://doi.org/10.1186/s13021-022-00214-w

Bloom, A. A., Bowman, K. W., Lee, M., Turner, A. J., Schroeder, R., Worden, J. R., et al. (2017). A global wetland methane emissions and uncertainty dataset for atmospheric chemical transport models (WetCHARTs version 1.0). *Geoscientific Model Development*, *10*(6), 2141–2156. https://doi.org/10.5194/gmd-10-2141-2017

Bouwman, A. F. (1996). Direct emission of nitrous oxide from agricultural soils. *Nutrient Cycling in Agroecosystems*, *46*(1), 53–70. https://doi.org/10.1007/BF00210224

Canadell, J. G., Ciais, P., Gurney, K., Le Quéré, C., Piao, S., Raupach, M. R., & Sabine, C. L. (2011). An international effort to quantify regional carbon fluxes. *Eos, Transactions American Geophysical Union*, *92*(10), 81–82. https://doi.org/10.1029/2011eo100001

Canadell, J. G., Monteiro, P. M., Costa, M. H., Da Cunha, L. C., Cox, P. M., Alexey, V., et al. (2021). Global carbon and other biogeochemical cycles and feedbacks. In *IPCC AR6 WGI, final Government distribution, chapter 5*.

Caro, D., Davis, S. J., Bastianoni, S., & Caldeira, K. (2014). Global and regional trends in greenhouse gas emissions from livestock. *Climatic Change*, *126*(1–2), 203–216. https://doi.org/10.1007/s10584-014-1197-x

Chandra, N., Patra, P. K., Bisht, J. S. H., Ito, A., Umezawa, T., Saigusa, N., et al. (2021). Emissions from the oil and gas sectors, coal mining and ruminant farming drive methane growth over the past three decades. *Journal of the Meteorological Society of Japan. Ser. II*, *99*(2), 309–337. https://doi.org/10.2151/jmsj.2021-015

Chang, Z., Fan, L., Wigneron, J.-P., Wang, Y.-P., Ciais, P., Chave, J., et al. (2023). Estimating aboveground carbon dynamic of China using optical and microwave remote-sensing datasets from 2013 to 2019. *Journal of Remote Sensing*, *3*, 0005. https://doi.org/10.34133/remotesensing.0005

Chen, B., Zhang, H., Wang, T., & Zhang, X. (2021). An atmospheric perspective on the carbon budgets of terrestrial ecosystems in China: Progress and challenges. *Science Bulletin*, *66*(17), 1713–1718. https://doi.org/10.1016/j.scib.2021.05.017

Chen, C., Park, T., Wang, X., Piao, S., Xu, B., Chaturvedi, R. K., et al. (2019). China and India lead in greening of the world through land-use management. *Nature Sustainability*, *2*(2), 122–129. https://doi.org/10.1038/s41893-019-0220-7

Chen, H., Zhu, Q., Peng, C., Wu, N., Wang, Y., Fang, X., et al. (2013). Methane emissions from rice paddies natural wetlands, and lakes in China: Synthesis and new estimate. *Global Change Biology*, *19*(1), 19–32. https://doi.org/10.1111/gcb.12034

Chini, L., Hurtt, G., Sahajpal, R., Frolking, S., Klein Goldewijk, K., Sitch, S., et al. (2021). Land-use harmonization datasets for annual global carbon budgets. *Earth System Science Data*, *13*(8), 4175–4189. https://doi.org/10.5194/essd-13-4175-2021

Ciais, P., Bastos, A., Chevallier, F., Lauerwald, R., Poulter, B., Canadell, P., et al. (2022). Definitions and methods to estimate regional land carbon fluxes for the second phase of the REgional Carbon Cycle Assessment and Processes Project (RECCAP-2). *Geoscientific Model Development*. https://doi.org/10.5194/gmd-2020-259

Ciais, P., Tan, J., Wang, X., Roedenbeck, C., Chevallier, F., Piao, S. L., et al. (2019). Five decades of northern land carbon uptake revealed by the interhemispheric CO(2) gradient. *Nature*, *568*(7751), 221–225. https://doi.org/10.1038/s41586-019-1078-6

Ciais, P., Yao, Y., Gasser, T., Baccini, A., Wang, Y., Lauerwald, R., et al. (2021). Empirical estimates of regional carbon budgets imply reduced global soil heterotrophic respiration. *National Science Review*, *8*(2). https://doi.org/10.1093/nsr/nwaa145

Crippa, M., Guizzardi, D., Banja, M., Solazzo, E., Muntean, M., Schaaf, E., et al. (2022). *CO2 emissions of all world countries*. JRC/IEA/PBL 2022 Report, EUR 31182 EN. Publications Office of the European Union. Retrieved from https://www.ncbi.nlm.nih.gov/pubmed/34660638

Cui, X., Shang, Z., Xia, L., Xu, R., Adalibieke, W., Zhan, X., et al. (2022). Deceleration of cropland-N2O emissions in China and future mitigation potentials. *Environmental Science and Technology*, *56*(7), 4665–4675. https://doi.org/10.1021/acs.est.1c07276

Cui, X., Zhou, F., Ciais, P., Davidson, E. A., Tubiello, F. N., Niu, X., et al. (2021). Global mapping of crop-specific emission factors highlights hotspots of nitrous oxide mitigation. *Nature Food*, *2*(11), 886–893. https://doi.org/10.1038/s43016-021-00384-9

Dong, B., Xi, Y., Cui, Y., & Peng, S. (2023). Quantifying methane emissions from aquaculture ponds in China. *Environmental Science and Technology*, *57*(4), 1576–1583. https://doi.org/10.1021/acs.est.2c05218

EPA. (2021). A data exploration tool for viewing non-CO_2 GHG projections and mitigation assessments from the United Stated Environmental Protection Agency. Retrieved from https://cfpub.epa.gov/ghgdata/nonco2/

Etiope, G., Ciotoli, G., Schwietzke, S., & Schoell, M. (2019). Gridded maps of geological methane emissions and their isotopic signature. *Earth System Science Data*, *11*(1), 1–22. https://doi.org/10.5194/essd-11-1-2019

FAO. (2021). Emissions from agriculture and forest land. Global, regional and country trends 1990–2019. In *FAOSTAT analytical brief series* (Vol. 25). Retrieved from http://www.fao.org/faostat/en/#data/GT

FAO. (2022). World food and agriculture—Statistical pocketbook 2022. https://doi.org/10.4060/cc2212en

Friedlingstein, P., O'Sullivan, M., Jones, M. W., Andrew, R. M., Gregor, L., Hauck, J., et al. (2022). Global carbon budget 2022. *Earth System Science Data*, *14*(11), 4811–4900. https://doi.org/10.5194/essd-14-4811-2022

Gasser, T., Crepin, L., Quilcaille, Y., Houghton, R. A., Ciais, P., & Obersteiner, M. (2020). Historical CO_2 emissions from land use and land cover change and their uncertainty. *Biogeosciences*, *17*(15), 4075–4101. https://doi.org/10.5194/bg-17-4075-2020

Gilfillan, D., & Marland, G. (2021). CDIAC-FF: Global and national CO_2 emissions from fossil fuel combustion and cement manufacture: 1751–2017. *Earth System Science Data*, *13*(4), 1667–1680. https://doi.org/10.5194/essd-13-1667-2021

GIR. (2021). *Gir: Greenhouse gas inventory and research center, 2021 national greenhouse gas emission statistics of Republic of Korea*. Greenhouse Gas Inventory and Research Center. Retrieved from http://www.gir.go.kr/home/index.do?menuId=36

GRiSP (Global Rice Science Partnership) Rice Almanac. (2013). *GRiSP (global rice science partnership) rice almanac* (4th ed.). International Rice Research Institute.

Gu, B., Zhang, X., Lam, S. K., Yu, Y., van Grinsven, H. J. M., Zhang, S., et al. (2023). Cost-effective mitigation of nitrogen pollution from global croplands. *Nature*, *613*(7942), 77–84. https://doi.org/10.1038/s41586-022-05481-8

Gütschow, J., Günther, A., & Pflüger, M. (2021). The PRIMAP-hist national historical emissions time series (1750-2019) v2.3.1 (2.3.1).

Gütschow, J., Jeffery, M. L., Gieseke, R., Gebel, R., Stevens, D., Krapp, M., & Rocha, M. (2016). The PRIMAP-hist national historical emissions time series. *Earth System Science Data*, *8*(2), 571–603. https://doi.org/10.5194/essd-8-571-2016

Hansis, E., Davis, S. J., & Pongratz, J. (2015). Relevance of methodological choices for accounting of land use change carbon fluxes. *Global Biogeochemical Cycles*, *29*(8), 1230–1246. https://doi.org/10.1002/2014GB004997

Hartmann, J., Jansen, N., Dürr, H. H., Kempe, S., & Köhler, P. (2009). Global CO_2-consumption by chemical weathering: What is the contribution of highly active weathering regions? *Global and Planetary Change*, *69*(4), 185–194. https://doi.org/10.1016/j.gloplacha.2009.07.007

Hayashi, K., Shibata, H., Oita, A., Nishina, K., Ito, A., Katagiri, K., et al. (2021). Nitrogen budgets in Japan from 2000 to 2015: Decreasing trend of nitrogen loss to the environment and the challenge to further reduce nitrogen waste. *Environmental Pollution*, *286*, 117559. https://doi.org/10.1016/j.envpol.2021.117559

Hoesly, R. M., Smith, S. J., Feng, L., Klimont, Z., Janssens-Maenhout, G., Pitkanen, T., et al. (2018). Historical (1750–2014) anthropogenic emissions of reactive gases and aerosols from the Community Emissions Data System (CEDS). *Geoscientific Model Development*, *11*(1), 369–408. https://doi.org/10.5194/gmd-11-369-2018

Houghton, R. A., & Nassikas, A. A. (2017). Global and regional fluxes of carbon from land use and land cover change 1850-2015. *Global Biogeochemical Cycles*, *31*(3), 456–472. https://doi.org/10.1002/2016gb005546

Hu, Z., Lee, J. W., Chandran, K., Kim, S., & Khanal, S. K. (2012). Nitrous oxide (N_2O) emission from aquaculture: A review. *Environmental Science and Technology*, *46*(12), 6470–6480. https://doi.org/10.1021/es300110x

IPCC. (2006). Intergovernmental panel on climate change (IPCC) guidelines for national greenhouse gas inventories. Volume 4. In *Agriculture, forestry and other land uses*. Intergovernmental Panel on Climate Change. Retrieved from https://www.ipcc-nggip.iges.or.jp/public/2006gl/vol4.html

IPCC. (2019). Intergovernmental panel on climate change (IPCC) guidelines for national greenhouse gas inventories. Volume 4. *Agriculture, forestry and other land uses*. Intergovernmental Panel on Climate Change.Retrieved from https://www.ipcc-nggip.iges.or.jp/public/2019rf/vol4.html. https://www.ipcc-nggip.iges.or.jp/public/2019rf/vol4.html

IPCC. (2021). Summary for policymakers. In *Climate change 2021: The physical science basis. Contribution of Working Group I to the Sixth Assessment Report of the Intergovernmental Panel on Climate Change*. Retrieved from https://www.ipcc.ch/report/ar6/wg1/chapter/summary-for-policymakers/

IPCC. (2022). In P. R. Shukla, J. Skea, R. Slade, A. Al Khourdajie, R. van Diemen, et al. (Eds.), *Climate change 2022: Mitigation of climate change. Contribution of working group III to the sixth assessment report of the intergovernmental panel on climate change*. Cambridge University Press. https://doi.org/10.1017/9781009157926

Ito, A. (2021). Bottom-up evaluation of the regional methane budget of northern lands from 1980 to 2015. *Polar Science*, *27*, 100558. https://doi.org/10.1016/j.polar.2020.100558

Ito, A., Nishina, K., Ishijima, K., Hashimoto, S., & Inatomi, M. (2018). Emissions of nitrous oxide (N2O) from soil surfaces and their historical changes in East Asia: A model-based assessment. *Progress in Earth and Planetary Science*, *5*(1), 55. <Go to ISI>://WOS:000446253600001. https://doi.org/10.1186/s40645-018-0215-4

Ito, A., Tohjima, Y., Saito, T., Umezawa, T., Hajima, T., Hirata, R., et al. (2019). Methane budget of East Asia, 1990-2015: A bottom-up evaluation. *Science of the Total Environment*, *676*, 40–52. https://doi.org/10.1016/j.scitotenv.2019.04.263

Jiang, F., Chen, J. M., Zhou, L., Ju, W., Zhang, H., Machida, T., et al. (2016). A comprehensive estimate of recent carbon sinks in China using both top-down and bottom-up approaches. *Scientific Reports*, *6*(1), 22130. https://doi.org/10.1038/srep22130

Kumari, S., Fagodiya, R. K., Hiloidhari, M., Dahiya, R. P., & Kumar, A. (2020). Methane production and estimation from livestock husbandry: A mechanistic understanding and emerging mitigation options. *Science of the Total Environment*, *709*, 136135. https://doi.org/10.1016/j.scitotenv.2019.136135

Lauerwald, R., Allen, G. H., Deemer, B. R., Liu, S., Maavara, T., Raymond, P., et al. (2023). Inland water greenhouse gas budgets for RECCAP2: 2. Regionalization and homogenization of estimates. *Global Biogeochemical Cycles*, *37*(5), e2022GB007658. https://doi.org/10.1029/2022GB007658

Long, Y., Yoshida, Y., Zhang, H., Zheng, H., Shan, Y., & Guan, D. (2020). Japan prefectural emission accounts and socioeconomic data 2007 to 2015. *Scientific Data*, *7*(1), 233. https://doi.org/10.1038/s41597-020-0571-y

Luo, Y., Keenan, T. F., & Smith, M. (2015). Predictability of the terrestrial carbon cycle. *Global Change Biology*, *21*(5), 1737–1751. https://doi.org/10.1111/gcb.12766

Mayorga, E., Seitzinger, S. P., Harrison, J. A., Dumont, E., Beusen, A. H. W., Bouwman, A. F., et al. (2010). Global nutrient export from WaterSheds 2 (NEWS 2): Model development and implementation. *Environmental Modelling & Software*, *25*(7), 837–853. https://doi.org/10.1016/j.envsoft.2010.01.007

McDuffie, E. E., Smith, S. J., O'Rourke, P., Tibrewal, K., Venkataraman, C., Marais, E. A., et al. (2020). A global anthropogenic emission inventory of atmospheric pollutants from sector- and fuel-specific sources (1970–2017): An application of the community emissions data system (CEDS). *Earth System Science Data*, *12*(4), 3413–3442. https://doi.org/10.5194/essd-12-3413-2020

Messager, M. L., Lehner, B., Grill, G., Nedeva, I., & Schmitt, O. (2016). Estimating the volume and age of water stored in global lakes using a geo-statistical approach. *Nature Communications*, *7*(1), 13603. https://doi.org/10.1038/ncomms13603

NCCC. (2010). The second national communication on climate change of the People's Republic of China, the People's Republic of China.

NCCC. (2018). The third national communication on climate change of the People's Republic of China, the People's Republic of China.

NIES. (2022). *National greenhouse gas inventory report of Japan*. Ministry of the Environment, Japan Greenhouse Gas Inventory Office of Japan (GIO), CGER, NIES.

Oita, A., Nagano, I., & Matsuda, H. (2018). Food nitrogen footprint reductions related to a balanced Japanese diet. *Ambio*, *47*(3), 318–326. https://doi.org/10.1007/s13280-017-0944-4

Peters, G. P., Davis, S. J., & Andrew, R. (2012). A synthesis of carbon in international trade. *Biogeosciences*, *9*(8), 3247–3276. https://doi.org/10.5194/bg-9-3247-2012

Piao, S., He, Y., Wang, X., & Chen, F. (2022). Estimation of China's terrestrial ecosystem carbon sink: Methods, progress and prospects. *Science China Earth Sciences*, *65*(4), 641–651. https://doi.org/10.1007/s11430-021-9892-6

Piao, S., Huang, M. T., Liu, Z., Wang, X. H., Ciais, P., Canadell, J. G., et al. (2018). Lower land-use emissions responsible for increased net land carbon sink during the slow warming period. *Nature Geoscience*, *11*(10), 739–743. https://doi.org/10.1038/s41561-018-0204-7

Piao, S., Ito, A., Li, S. G., Huang, Y., Ciais, P., Wang, X. H., et al. (2012). The carbon budget of terrestrial ecosystems in East Asia over the last two decades. *Biogeosciences*, *9*(9), 3571–3586. https://doi.org/10.5194/bg-9-3571-2012

Pugh, T. A. M., Lindeskog, M., Smith, B., Poulter, B., Arneth, A., Haverd, V., & Calle, L. (2019). Role of forest regrowth in global carbon sink dynamics. *Proceedings of the National Academy of Sciences of the United States of America*, *116*(10), 4382–4387. https://doi.org/10.1073/pnas.1810512116

Qiu, J. (2009). China cuts methane emissions from rice fields. *Nature*. https://doi.org/10.1038/news.2009.833

Saunois, M., Stavert, A. R., Poulter, B., Bousquet, P., Canadell, J. G., Jackson, R. B., et al. (2020). The global methane budget 2000–2017. *Earth System Science Data*, *12*(3), 1561–1623. https://doi.org/10.5194/essd-12-1561-2020

Shan, Y., Guan, D., Zheng, H., Ou, J., Li, Y., Meng, J., et al. (2018). China CO_2 emission accounts 1997–2015. *Scientific Data*, *5*(1), 170201. https://doi.org/10.1038/sdata.2017.201

Shan, Y., Huang, Q., Guan, D., & Hubacek, K. (2020). China CO_2 emission accounts 2016–2017. *Scientific Data*, *7*(1), 54. https://doi.org/10.1038/s41597-020-0393-y

Stavert, A. R., Saunois, M., Canadell, J. G., Poulter, B., Jackson, R. B., Regnier, P., et al. (2021). Regional trends and drivers of the global methane budget. *Global Change Biology*, *28*(1), 182–200. https://doi.org/10.1111/gcb.15901

Stephens, B. B., Gurney, K. R., Tans, P. P., Sweeney, C., Peters, W., Bruhwiler, L., et al. (2007). Weak northern and strong tropical land carbon uptake from vertical profiles of atmospheric CO_2. *Science*, *316*(5832), 1732–1735. https://doi.org/10.1126/science.1137004

Tagesson, T., Schurgers, G., Horion, S., Ciais, P., Tian, F., Brandt, M., et al. (2020). Recent divergence in the contributions of tropical and boreal forests to the terrestrial carbon sink. *Nature Ecology & Evolution*, *4*(2), 202–209. https://doi.org/10.1038/s41559-019-1090-0

Thompson, R. L., Lassaletta, L., Patra, P. K., Wilson, C., Wells, K. C., Gressent, A., et al. (2019). Acceleration of global N_2O emissions seen from two decades of atmospheric inversion. *Nature Climate Change*, *9*(12), 993–998. <Go to ISI>://WOS:000499106300027. https://doi.org/10.1038/s41558-019-0613-7

Thompson, R. L., Stohl, A., Zhou, L. X., Dlugokencky, E., Fukuyama, Y., Tohjima, Y., et al. (2015). Methane emissions in East Asia for 2000-2011 estimated using an atmospheric Bayesian inversion. *Journal of Geophysical Research: Atmospheres*, *120*(9), 4352–4369. https://doi.org/10.1002/2014jd022394

Tian, H., Lu, C., Ciais, P., Michalak, A. M., Canadell, J. G., Saikawa, E., et al. (2016). The terrestrial biosphere as a net source of greenhouse gases to the atmosphere. *Nature*, *531*(7593), 225–228. https://doi.org/10.1038/nature16946

Tian, H., Xu, R., Canadell, J. G., Thompson, R. L., Winiwarter, W., Suntharalingam, P., et al. (2020). A comprehensive quantification of global nitrous oxide sources and sinks. *Nature*, *586*(7828), 248–256. https://doi.org/10.1038/s41586-020-2780-0

Tian, H., Yang, J., Lu, C., Xu, R., Canadell, J. G., Jackson, R. B., et al. (2018). The global N_2O model intercomparison project. *Bulletin of the American Meteorological Society*, *99*(6), 1231–1251. https://doi.org/10.1175/bams-d-17-0212.1

Tubiello, F. N. (2019). Greenhouse gas emissions due to agriculture. In P. Ferranti, E. M. Berry, & J. R. Anderson (Eds.), *Encyclopedia of food security and sustainability* (pp. 196–205). Elsevier.

Van Der Werf, G. R., Randerson, J. T., Giglio, L., van Leeuwen, T. T., Chen, Y., Rogers, B. M., et al. (2017). Global fire emissions estimates during 1997–2016. *Earth System Science Data*, *9*(2), 697–720. https://doi.org/10.5194/essd-9-697-2017

Wang, Q., Zhou, F., Shang, Z., Ciais, P., Winiwarter, W., Jackson, R. B., et al. (2020). Data-driven estimates of global nitrous oxide emissions from croplands. *National Science Review*, *7*(2), 441–452. https://doi.org/10.1093/nsr/nwz087

Wang, Y., Wang, X., Wang, K., Chevallier, F., Zhu, D., Lian, J., et al. (2022). The size of the land carbon sink in China. *Nature*, *603*(7901), E7–E9. https://doi.org/10.1038/s41586-021-04255-y

Xu, L., Saatchi, S. S., Yang, Y., Yu, Y., Pongratz, J., Bloom, A. A., et al. (2021). Changes in global terrestrial live biomass over the 21st century. *Science Advances*, *7*(27), eabe9829. https://doi.org/10.1126/sciadv.abe9829

Xu, P., Houlton, B. Z., Zheng, Y., Zhou, F., Ma, L., Li, B., et al. (2022). Policy-enabled stabilization of nitrous oxide emissions from livestock production in China over 1978–2017. *Nature Food*, *3*(5), 356–366. https://doi.org/10.1038/s43016-022-00513-y

Xu, P., Liao, Y., Zheng, Y., Zhao, C., Zhang, X., Zheng, Z., & Luan, S. (2019). Northward shift of historical methane emission hotspots from the livestock sector in China and assessment of potential mitigation options. *Agricultural and Forest Meteorology*, *272*, 1–11. https://doi.org/10.1016/j.agrformet.2019.03.022

Yan, Y., Lauerwald, R., Wang, X., Regnier, P., Ciais, P., Ran, L., et al. (2023). Increasing riverine export of dissolved organic carbon from China. *Global Change Biology*, *29*(17), 5014–5032. https://doi.org/10.1111/gcb.16819

Yu, C., Huang, X., Chen, H., Godfray, H. C. J., Wright, J. S., Hall, J. W., et al. (2019). Managing nitrogen to restore water quality in China. *Nature*, *567*(7749), 516–520. https://doi.org/10.1038/s41586-019-1001-1

Yu, G., Jia, Y., He, N., Zhu, J., Chen, Z., Wang, Q., et al. (2019). Stabilization of atmospheric nitrogen deposition in China over the past decade. *Nature Geoscience*, *12*(6), 424–429. https://doi.org/10.1038/s41561-019-0352-4

Yu, Z., Ciais, P., Piao, S., Houghton, R. A., Lu, C., Tian, H., et al. (2022). Forest expansion dominates China's land carbon sink since 1980. *Nature Communications*, *13*(1), 5374. https://doi.org/10.1038/s41467-022-32961-2

Yuan, J., Xiang, J., Liu, D., Kang, H., He, T., Kim, S., et al. (2019). Rapid growth in greenhouse gas emissions from the adoption of industrial-scale aquaculture. *Nature Climate Change*, *9*(4), 318–322. https://doi.org/10.1038/s41558-019-0425-9

Yue, X., Liao, H., Wang, H., Zhang, T., Unger, N., Sitch, S., et al. (2020). Pathway dependence of ecosystem responses in China to 1.5°C global warming. *Atmospheric Chemistry and Physics*, *20*(4), 2353–2366. https://doi.org/10.5194/acp-20-2353-2020

Zhang, B., Tian, H., Ren, W., Tao, B., Lu, C., Yang, J., et al. (2016). Methane emissions from global rice fields: Magnitude, spatiotemporal patterns, and environmental controls. *Global Biogeochemical Cycles*, *30*(9), 1246–1263. https://doi.org/10.1002/2016gb005381

Zhang, L., Tian, H., Shi, H., Pan, S., Qin, X., Pan, N., & Dangal, S. R. S. (2021). Methane emissions from livestock in East Asia during 1961-2019. *Ecosystem Health and Sustainability*, *7*(1). https://doi.org/10.1080/20964129.2021.1918024

Zhang, Y., Fang, S., Chen, J., Lin, Y., Chen, Y., Liang, R., et al. (2022a). Observed changes in China's methane emissions linked to policy drivers. *Proceedings of the National Academy of Sciences of the United States of America*, *119*(41), e2202742119. https://doi.org/10.1073/pnas.2202742119

Zhang, Y., Tang, K. W., Yang, P., Yang, H., Tong, C., Song, C., et al. (2022). Assessing carbon greenhouse gas emissions from aquaculture in China based on aquaculture system types, species, environmental conditions and management practices. *Agriculture, Ecosystems & Environment*, 338.

Zhang, Z., Fluet-Chouinard, E., Jensen, K., McDonald, K., Hugelius, G., Gumbricht, T., et al. (2021b). Development of the global dataset of wetland area and dynamics for methane modeling (WAD2M). *Earth System Science Data*, *13*(5), 2001–2023. https://doi.org/10.5194/essd-13-2001-2021

Zhou, Y., Huang, M., Tian, H., Xu, R., Ge, J., Yang, X., et al. (2021). Four decades of nitrous oxide emission from Chinese aquaculture underscores the urgency and opportunity for climate change mitigation. *Environmental Research Letters*, *16*(11), 114038. https://doi.org/10.1088/1748-9326/ac3177

References From the Supporting Information

Ciais, P., Bastos, A., Chevallier, F., Lauerwald, R., Poulter, B., Canadell, P., et al. (2020). Definitions and methods to estimate regional land carbon fluxes for the second phase of the REgional Carbon Cycle Assessment and Processes Project (RECCAP-2). *Geoscientific Model Development*. https://doi.org/10.5194/gmd-2020-259

Dong, X., Anderson, N. J., Yang, X., chen, X., & Shen, J. (2012). Carbon burial by shallow lakes on the Yangtze floodplain and its relevance to regional carbon sequestration. *Global Change Biology*, *18*(7), 2205–2217. https://doi.org/10.1111/j.1365-2486.2012.02697.x

Gui, Z.-F., Xue, B., Yao, S.-C., Wei, W.-J., & Yi, S. (2013). Organic carbon burial in lake sediments in the middle and lower reaches of the Yangtze River Basin, China. *Hydrobiologia*, *710*(1), 143–156. https://doi.org/10.1007/s10750-012-1365-9

Lauerwald, R., Regnier, P., Figueiredo, V., Enrich-Prast, A., Bastviken, D., Lehner, B., et al. (2019). Natural lakes are a minor global source of N_2O to the atmosphere. *Global Biogeochemical Cycles*, *33*(12), 1564–1581. ADDIN EN.CITE ADDIN EN.CITE.DATA. https://doi.org/10.1029/2019GB006261

Maavara, T., Lauerwald, R., Laruelle, G. G., Akbarzadeh, Z., Bouskill, N. J., Van Cappellen, P., & Regnier, P. (2019). Nitrous oxide emissions from inland waters: Are IPCC estimates too high? *Global Change Biology*, *25*(2), 473–488. https://doi.org/10.1111/gcb.14504

Marzadri, A., Amatulli, G., Tonina, D., Bellin, A., Shen, L. Q., Allen, G. H., & Raymond, P. A. (2021). Global riverine nitrous oxide emissions: The role of small streams and large rivers. *Science of the Total Environment*, *776*, 145148. https://doi.org/10.1016/j.scitotenv.2021.145148